Final Report

Specific targeting of MUC1 overexpressing breast carcinoma cells with anti-cancer drug-loaded nanoparticles

By Supang Khondee

June 2016

Contract No. TRG5780051

Final Report

Specific targeting of MUC1 overexpressing breast carcinoma cells with anti-cancer drug-loaded nanoparticles

	Researcher	Institute
1.	Supang Khondee	University of Phayao
2.	Chuda Chittasupho	Srinakharinwirot University
3.	Singkome Tima	Chiang Mai University
4.	Songyot Anuchapreeda	Chiang Mai University

1. Abstract

Project Code : TRG5780051

Project Title : Specific targeting of MUC1 overexpressing breast carcinoma cells with anti-cancer drug-loaded nanoparticles

Investigator : Supang Khondee

E-mail Address : s.khondee@gmail.com

Project Period : 2 year (June 2, 2014 to June 1, 2016)

บทคัดย่อ:

มะเร็งเต้านมเป็นมะเร็งที่เป็นสาเหตุหลักของการตายจากมะเร็งในผู้หญิงทั่วโลก โปรตีนมิวซิน1 เป็น โปรตีนที่มีการแสดงออกสูงถึงร้อยละ 90 ในมะเร็งเต้านม การศึกษานี้ตั้งเป้าเพื่อที่จะผลิตไมเซลล์ที่บรรจุยารักษามะเร็งด็อกโซรูบิซิน เพื่อที่จะนำส่งยาอย่างเฉพาะเจาะจงไปที่เซลล์มะเร็งที่แสดงออกโปรตีนมิวซิน อนุภาคนาโนชนิดไมเซลล์ถูกสร้างจากการจัดเรียงตัวเองของโคโพลิเมอร์เพกกีเลทออกตะเดซิลลิโธโคเลทในตัวกลางที่เป็นน้ำ เปบไทด์ที่จับแบบเฉพาะเจาะจงกับโปรตีนมิวซิน1 ได้แก่ QND และ HSQ เปบไทด์ ถูกสังเคราะห์ ทดสอบการจับแบบเฉพาะเจาะจงกับเซลล์มะเร็งที่แสดงออกโปรตีนมิวซิน และนำมาเชื่อมต่อบนผิวของไมเซลล์ ขนาดของไมเซลล์แบบธรรมดา QND และ HSQ ไมเซลล์ที่บรรจุยาดอกโซรูบิซิน คือ 320 300 และ 319 นาโนเมตร ตามลำดับ โดยมีความสามารถในการกักเก็บยาด็อกโซรูบิซินได้ร้อยละ 71 86 และ 93 ตามลำดับ ไมเซลล์แบบธรรมดา QND และ HSQ ไมเซลล์ มีค่าความเข้มข้นวิกฤติในการจัดเรียงตัวเป็นไมเซลล์ คือ 110.5 55.1 และ 98.9 ไมโครโมลาร์ ตามลำดับ จากนั้นได้ทำการทดสอบการปลดปล่อยยาดอกโซรูบิซินจากไมเซลล์ในสารละลายบัฟเฟอร์พีเอช 7 โดยไมเซลล์แบบธรรมดา QND และ HSQ ไมเซลล์ ปลดปล่อยตัวยาออกมาร้อยละ 13.1 15.8 และ 16.9 หลังจากทำการทดสอบ 4 ชั่วโมง ในสารละลายบัฟเฟอร์พีเอช 7 ค่าความเข้มข้นในการยับยั้งการเติบโตของเซลล์มะเร็งได้ร้อยละ 50 ของไมเซลล์แบบธรรมดา QND และ HSQ ไมเซลล์ที่บรรจุยาดอกโซรูบิซิน มีค่าไม่แตกต่างจากค่าความเข้มข้นในการยับยั้งการเติบโตของเซลล์มะเร็งได้ร้อยละ 50 ของยาด็อกโซรูบิซิน นอกจากนี้ เราได้ทดสอบการจับแบบเฉพาะเจาะจงและการนำไมเซลล์เข้าสู่เซลล์มะเร็ง พบว่า QND และ HSQ ไมเซลล์จับแบบเฉพาะเจาะจงกับเซลล์มะเร็งเต้านม BT549-Luc และ T47D และถูกนำเข้าสู่เซลล์ได้มากกว่าไมเซลล์แบบธรรมดาอย่างมีนัยสำคัญทางสถิติ จากผลการศึกษาดังกล่าว สามารถสรุปได้ว่า QND และ HSQ ไมเซลล์สามารถนำส่งยาด็อกโซรูบิซินไปสู่เซลล์มะเร็งได้อย่างเฉพาะเจาะจงและมีความเป็นไปได้สูงที่จะนำไปใช้ในการรักษามะเร็งเต้านมชนิด triple negative

คำสำคัญ : โปรตีนมิวซิน1 การรักษาแบบเฉพาะเจาะจง มะเร็งเต้านม ด็อกโซรูบิซิน ไมเซลล์

Abstract:

Breast cancer is the leading cause of cancer death among women. The human mucin1 protein (MUC1) is overexpressed in approximately 90% of human breast cancers. In order to increase therapeutic effect of a model drug, doxorubicin (DOX), on breast cancer, DOX loaded micelles that target MUC1 was developed. The micelle was self-assembled using copolymer pegylated octadecyl lithocholate as an amphiphilic platform. MUC1 targeting peptides, QND and HSQ, were identified and conjugated on micelles. The size and drug entrapment efficiency of untargeted, QND-DOX and HSQ-DOX micelles were 320, 300 and 319 nm and 71, 86 and 93%, respectively. Critical micelle concentration (CMC) of untargeted, QND, and HSQ micelle were 110.5, 55.1, and 98.9 μM, respectively. In 4 h, DOX was released 13.1, 15.8 and 16.9 %, respectively, from untargeted, QND-DOX and HSQ-DOX micelles in pH 7 buffer. The IC50 of QND-DOX and HSQ-DOX micelles on BT549-Luc and T47D cells were comparable to that of free DOX. Additionally, we observed significantly greater binding and uptake of QND-DOX and HSQ-DOX micelles on BT549-Luc and T47D cells compared to untargeted DOX micelle. These results suggested that QND-DOX and HSQ-DOX micelles had potential application in triple negative breast cancer treatment.

Keywords : human mucin1 protein (MUC1); targeted therapy; breast cancer; doxorubicin; micelles

2. Executive summary

In order to test our central hypothesis that nanoparticles loaded with anticancer drug that target MUC1 may offer improve breast cancer therapy, a model drug, doxorubicin (DOX), was encapsulated in micelles that target MUC1. The micelle was self-assembled using copolymer pegylated octadecyl lithocholate as an amphiphilic platform. The copolymer were synthesized in multiple steps. The copolymer synthesis reactions had yield vary from 62.3 to 91.9%. MUC1 targeting peptides, QND, HSQ, and TNT, were identified from previous study. They were synthesized manually via Fmoc standard solid phase peptide synthesis (SPPS) and labeled with a fluorescent dye, fluorescein isothiocyanate (FITC). The fluorescent peptides were purified using semi-preparative HPLC and had purity 84.7, 89.5, and 75.3%, respectively, on an analytical HPLC. The peptides were then evaluated specific binding on MUC1 expressing breast carcinoma cell lines, BT549-Luc and T47D. QND and HSQ peptides showed superior specific binding to BT549-Luc and T47D cells using fluorescent microscope followed by image analysis. Therefore, QND and HSQ peptides were chosen to be grafted on micelle surface to make MUC1 targeting micelle. QND and HSQ were synthesized again to have thiol functional group which will be used to conjugate to pegylated copolymer that have maleiimde functional group. Untargeted and MUC1 targeting micelles were then formulated and DOX was loaded onto micelles. The size and surface charge of untargeted DOX, QND-DOX and HSQ-DOX micelles were determined using dynamic light scattering (DLS). The hydrodynamic diameter and zeta potential (surface charge) of untargeted DOX, QND-DOX and HSQ-DOX micelles were 320, 300 and 319 nm and -3.0, 4.5, and 1.6 mV, respectively. Drug entrapment efficiency was assessed using a microplate reader. The entrapment efficiencies of untargeted DOX, QND-DOX and HSQ-DOX micelles were 71, 86 and 93%, respectively. Critical micelle concentration (CMC) of micelles were also examined using a fluorescent probe (pyrene) that emission spectra change according to

microenvironment. The CMC value of untargeted, QND, and HSQ micelle was 110.5, 55.1, and 98.9 μM, respectively. In addition, release profile of DOX from micelles was investigated using a microplate reader. In general, the release of DOX from drug carriers was pH dependent probably due to the increase in solubility of DOX at mildly acidic pH. However, release profile of DOX from micelles are similar in both pH 4 and pH 7 buffer. In 4 h, DOX was released 13.1, 15.8 and 16.9 %, respectively, from untargeted DOX, QND-DOX and HSQ-DOX micelles in pH 7 buffer. At the same period of time, DOX was released 12.3, 15.8 and 15.8 %, respectively, from untargeted DOX, QND-DOX and HSQ-DOX micelles in pH 4 buffer. This slow release phenomenon in both pH may due to high crystallinity of copolymer octadecyl lithocholate. The cytotoxicity of free DOX, untargeted DOX, QND-DOX, and HSQ-DOX micelles to BT549-Luc and T47D was evaluated by using MTT assay. Cytotoxicity of tested micelles was presented as the half maximal inhibitory concentration (IC50). At the concentration, the test substance inhibits cell viability by 50%. The IC50 of free DOX, untargeted DOX, QND-DOX and HSQ-DOX micelles on BT549-Luc was 4.3, 4.4, 1.75, and 3.75 μM, and was 5.2, 4.2, 4.6, and 4 μM on T47D cells, respectively. The relative IC50 value of DOX from each formulation were comparable to that of free DOX suggesting that the activity of drug encapsulated in micelles was not affected by the encapsulation process. Additionally, we observed significantly greater binding and uptake of QND-DOX and HSQ-DOX micelles on BT549-Luc and T47D cells compared to untargeted DOX micelle. These results suggested that QND-DOX and HSQ-DOX micelles had potential application in breast cancer treatment.

3. Objective

In this study, (1) we would like to identify MUC1 targeting peptides using both computational docking experiment and the specific binding of several MUC1 targeting peptides on MUC1 expressing breast cancer cell lines will be examined. (2) We also would like to formulate and characterize MUC1

targeting micelle. Therefore, the top two targeting peptides were then conjugated to micelle platform. DOX loaded targeting micelles will be formulated followed by size and surface charge, drug entrapment efficiency, release, and cytotoxicity assessments. (3) Additionally, we would like to evaluate targetability of the formulated micelle. The binding and uptake of DOX loaded targeting micelles will be then evaluated on BT549-Luc and T47D breast cancer cells.

4. Research methodology

Materials

Human breast carcinoma cells (BT549-Luc and T47D) were obtained from the ATCC (Manassas, VA). Dulbecco's modified Eagle's medium (DMEM) was obtained from GIBCO. Phosphate-buffered saline (PBS) was obtained from Amresco, and penicillin-streptomycin was obtained from Capricorn scientific. Fetal bovine serum (FBS) was obtained from PAA laboratories. BT549-Luc and T47D were grown in DMEM. Cells were maintained according to ATCC guidelines.

Lithocholic acid, N,N'-diisopropylcarbodiimde (DIC), N-hydroxysuccinimide (NHS), and pyrene were obtained from Sigma. Succinic anhydride, 4-(dimethylamino) pyridine (DMAP), N,N-diisopropylethylamine (DIEA) were obtained from Merck. Octadecyl amine and fluorescein isothiocyanate (FITC) were obtained from Acros. N-(3-dimethylaminopropyl)-N'-ethylcarbodiimide HCl (EDC) was obtained from Fluka. Tris (2-carboxyethyl) phosphine HCl (TCEP) was obtained from Thermo Scientific and 3-[4,5-dimethylthiazol-2-yl]-2,5 diphenyl tetrazolium bromide (MTT) was obtained from AppliChem. Doxorubicin was purchased from LC Laboratories. Methoxy PEG_{3K} amine and maleiimide $PEG_{3.5K}$ amine were obtained from JenKem Technology. Fmoc-amino acids, Boc amino acids, o-benzotriazole-N,N,N′,N′-tetramethyluronium hexafluorophosphate (HBTU) and 1-Hydroxybenzotriazole (HOBt) and rink amide MBHA resin were obtained from Aapptec. Dialysis

membranes with molecular weight cut off (MWCO) of 12-14 kDa were obtained from Spectrum Laboratories, Inc. All reagents were used as received.

Identification of peptides bound by MUC1 protein using computational methods

A computational pipeline to predict peptides that efficiently bind MUC1 protein was set up. In the pipeline, I-TASSER with default parameters was used to predict the structure of MUC1 protein. As a result, the software provided five MUC1 model structures, and the first model is usually the most accurate one. Thus, the first model was used as the structure of MUC1 protein in our study. In the same way, the structures of the candidate peptides was determined. Hex was used to infer the binding affinity between MUC1 protein and the candidate peptides, respectively. For each peptide, Hex docked it into the MUC1 structure based on Fast Fourier Transform (FFT), and calculated the *p*-value of the docking result. The *p*-value indicates how well the peptide and the protein fit each other. Thus, the p-value was used as a proxy of binding affinity between the peptide and the MUC1 structure.

Determination of MUC1 expression using western blot analysis

The expression level of MUC-1 protein (CD227) in various cell types was evaluated using Western blot analysis. The whole protein extracts from BT549-Luc and T47D cells were prepared using RIPA buffer (50 mM Tris-HCl, 150 mM NaCl, 1% Triton X-100, 0.5 mM ethylenediaminetetraacetic acid (EDTA), and 0.1% sodium dodecyl sulfate (SDS)) containing protease inhibitors. The protein concentration was measured by the Folin-Lowry method. Then, the proteins at 50 □g were separated by7.5% SDS-PAGE. The analysis for MUC-1 protein was performed using primary mouse anti-human MUC-1 (BioLegend Inc., San Diego, CA, USA) in the ratio 1:1000, followed by a treatment with HRP-conjugated anti-mouse IgG (Promaga, WI, USA) in the ratio 1:15000 dilution. The GAPDH protein was probed with primary rabbit polyclonal anti-GAPDH (Santa Cruz

Biotechnology, CA, USA) in the ratio 1:1000, followed by treatment with HRP-conjugated goat anti-rabbit IgG in a 1:20000 dilution (Promega, WI, USA). The protein bands were visualized using the Luminata Forte Western HRP substrate (Merck Millipore Corporation, MA, USA) and quantified by ChemiDoc XRS (Bio-Rad, CA, USA)

Synthesis and purification of fluorescence labeled MUC1 targeting peptides for in vitro peptide selection

The panel of candidate peptides (QNDRHPR-GGGSK, HSQLPQV-GGGSK and TNTLSNN-GGGSK) were synthesized manually using solid phase peptide synthesis with standard Fmoc chemistry. Fluorescein isothiocyanate (FITC) was conjugated at the C-terminus on the side chain of a lysine residue via the GGGSK linker. Resins (~0.03 mmol) were swelled in DMF (1 mL). In a separate tube, FITC (0.045 mmol) was dissolved in DMF (0.6 mL). ~23 μL of DIEA (46 μL, 0.26 mmol) was added to both tubes. FITC solution was added to the resins. The reaction was allowed to stir 2-3 days at room temperature. The resins were washed and cleaved. The resulting peptides were precipitated in cold diethyl ether. The peptides were then purified using a semi-preparative HPLC (Shimadzu) with water-acetonitrile gradient mobile phase containing 0.1% trifluoroacetic acid (TFA). The resulting peptides were lyophilized and characterized with an ESI mass spectrometer (MicrOTOF mass spectrometer, Bruker Daltonics). Peptides purity was determined on analytical HPLC.

Peptide synthesis for micelle conjugation

The QNDRHPR-GGGSC and HSQLPQV-GGGSC peptides were selected for micelle labeling, and synthesized as described above. At C terminal, cysteine (C) was introduced to make free thiol group after cleavation. This thiol group is for conjugation to maleiimide PEG octadecyl lithocholate to form peptide-copolymer conjugate. Resins were washed, cleaved, and the resulting peptide was

precipitated in cold diethyl ether. The resulting peptides were lyophilized. The peptide was then purified using a semi-preparative HPLC and characterized with an ESI mass spectrometer.

Fluorescence microscopy study of binding and uptake of QND, HSQ and TNT peptides

BT549-Luc cells were seeded in cell culture chamber slide and incubated overnight to allow cell attachment. The culture medium was removed and washed one time with PBS. The cells were incubated with 0.5% BSA in PBS for 30 min at 4°C to block non-specific binding. The cells were then incubated with FITC conjugated QND, HSQ and TNT peptides dissolved in serum-free DMEM for 60 min at 37 $^{\circ}$C, 5% CO_2 and were washed three times with PBS to remove unbound peptides. The cells were fixed in 4% paraformaldehyde. To visualize nuclei, cells were incubated with 2 μg/ml Hoechst33342 for 15 min at room temperature, washed three times with PBS, and examined under fluorescence microscope. Fluorescence micrographs were acquired using Nikon Eclipse TS100-F and NIS-Elements, version 4.0 software.

Synthesis of micelles

Octadecyl lithocholate

Lithocholic acid (1.5 g, 4 mmol) and HOBt (1.5 g, 10 mmol) were dissolved in N,N-dimethylformamide (DMF) (12 mL). DIC (1.5 mL, 10 mmol) was added. After 10 min for activation, octadecyl amine (0.9 g, 3.3 mmol) was added along with dichloromethane (DCM) 4 mL, and the reaction was allowed to stir overnight at room temperature (RT). The resulting product was filtered and vacuum dried.

Succinyl octadecyl lithocholate

Octadecyl lithocholate (573 mg, 0.91 mmol) was dissolved in anhydrous DCM (15 mL). Catalytic amount of DMAP was added. Succinic anhydride (90.9 mg, 0.91 mmol) and DIEA (950 μL,

5.45 mmol) were then added and the reaction was allowed to run overnight at RT. The solvent was evaporated under N_2 and the resulting product was vacuum dried.

Pegylated octadecyl lithocholate

Succinyl octadecyl lithocholate (128 mg, 0.18 mmol) was dissolved in DCM 2.5 ml and DMF 1 mL. HOBt (78 mg, 0.54 mmol) was added, following by adding DIC (84 μL, 0.54 mmol). Methoxy PEG amine (300 mg, 0.1 mmol) was added after 10 min for activation. The reaction was allowed to stir overnight at 40^{o}C. The solvent was partially removed under N_2 and the resulting product was precipitated in cold diethyl ether, centrifuged, and vacuum dried. Succinyl octadecyl lithocholate was conjugated with maleimide PEG amine in the same manner.

Thiol peptide and maleimide pegylated octadecyl lithocholate conjugation

Maleimide pegylated octadecyl lithocholate (335 mg, 0.08 mmol) and TCEP (19 mg, 0.07 mmol) were dissolved in phosphate buffer pH 8.0 (15 mL). Thiol peptide (0.07 mmol) was added and the reaction was allowed to run overnight at RT. The resulting product was dialyzed against three changes of water and lyophilized.

Fourier Transform Infrared (FTIR) spectrometry

FTIR spectra were recorded on a FT-IR spectrometer (Nicolet iS5, Thermo Scientific) to monitor changes in chemical structure of polymer conjugates. Samples were prepared in potassium bromide (KBr) discs and spectra were recorded in the range of 4000-400 cm^{-1}.

Micelle preparation

The micelles were prepared by dissolving pegylated octadecyl lithocholate and/or QND pegylated octadecyl lithocholate or HSQ pegylated octadecyl lithocholate in PBS. For targeted micelle, optimal peptide density (50%) was selected to present on micelle surface based on previous studies[21,

[22]. Polymers were sonicated ~30 min or until fully dispersed. Doxorubicin (10 mg/mL) basic stock solution was added to the polymer solution. DOX feeding amount was 1.5% w/w of polymer used. The solution was sonicated for 5 min. Then micelle solution was centrifuged at 8000 rpm for 10 min to remove insoluble material. Doxorubicin micelles in supernatant were separated. For all experiments, 1.6 mM of polymer was used.

Dynamic Light Scattering (DLS)

Hydrodynamic diameters and surface charges of micelles were determined on a Mavern nanosizer (Nano-ZS90) with a 4 mW linear polarized laser (633 nm He-Ne). Samples were studied at 25^{o}C and in 10 mm diameter polystyrene cells. The hydrodynamic diameters were calculated from the Stoked-Einstein equation. Measurements were made in triplicate with independently prepared samples, and variability was reported as ±standard deviation.

Transmission Electron Microscopy (TEM)

TEM images were obtained on a transmission electron microscope (JEOL JEM-2010). Samples were prepared onto copper grids with 1% uranyl acetate (negative staining).

Critical micelle concentration (CMC)

Micelles form spontaneously at the critical micelle concentration (CMC). Pyrene was dissolved in acetone (24 mM) and aliquots of stock solution were added to 1.5 mL eppendorf tubes to provide a final pyrene concentration of 6 μM. Acetone was evaporated and replaced with untargeted, QND, and HSQ micelles prepared with serial dilution (01.2-2450 μM). Solutions were incubated at 55^{o}C overnight and left at RT for 3 hours prior to the experiment. We measured the fluorescence intensity of pyrene at I_1 = 371 nm and I_3 = 383 nm over a range of concentrations of untargeted, QND, and HSQ micelles on a microplate reader.[23] The intensity ratios of I_1 to I_3 were plotted as a function of

logarithm of micelle concentration (log μM). The CMC value was taken from the intersection of the tangent to the curve at the inflection with the horizontal tangent through the points at concentrations.[24]

Entrapment efficiency (EE)

The amount of doxorubicin was determined by a microplate reader (Synergy H1, BioTek). Two hundred microliters of micelle solution was transferred to a black 96-well plate prior to reading. The entrapment efficiency (%EE) was calculated according to the following equation:

$$\text{Entrapment efficiency (\%EE)} = \frac{amount\ of\ encapsulated\ doxorubicin\ (\mu g)\ in\ micelles}{amount\ of\ added\ doxorubicin\ (\mu g)\ during\ formulation} \times 100.$$

Release study

The release of DOX from DOX loaded micelles was investigated by using dialysis method. Briefly, micelle solutions were prepared at concentration 1.6 mM. Doxorubicin was encapsulated ~1.5% (w/w) in micelles, and 3 mL of each formulation was transferred into 12,000 Da MWCO dialysis bag (Spectrum laboratories Inc.) (*n*=3). Dialysis bags were immerged in 100 mL of phosphate buffer at pH 7, and the release medium was stirred to facilitate drug release. The experiment was run at room temperature. At fixed time points, aliquots were taken, and drug concentrations were measured by a microplate reader. Release medium was added after each sampling.

Cytotoxicity

Cytotoxicity was determined by measuring growth inhibition for a panel of cells (BT549-Luc and T47D) on an MTT assay. Cell viability was calculated based on a comparison of untreated cells and those treated with free DOX and with DOX, QND-DOX, and HSQ-DOX micelles under the same conditions. The panel of cells were harvested and seeded at a density of 2.5×10^4 cells/well in 96-well plates. Cells were cultured for 24 hours prior to adding doxorubicin micelles in serial dilution. Free doxorubicin at equivalent doses was incubated with cells in the same manner. After 1 day of

incubation, the medium was removed, cells were washed twice with PBS, and MTT solution (10 μL, 5 mg/mL) was added to each well. After an additional 4 hours of incubation, MTT solution was removed. Formazan crystals produced by live cells were solubilized in DMSO and the absorbance was measured at 570 nm (test) and 630 nm (reference) using a microplate reader. Cytotoxicity of tested substance was presented as the half maximal inhibitory concentration (IC_{50}). At the concentration, the test substance inhibits cell viability by 50%.

Quantification of binding specificity and uptake of QND-DOX-micelles and HSQ-DOX-micelles

BT549-Luc and T47D cells were seeded in 96-well plate at a cell concentration of 80,000 cells/ml. QND-DOX-micelles and HSQ-DOX-micelles containing 16 μg/mL of DOX were suspended in serum free DMEM (2.5 mg/ml, 100 μl) and incubated with the cells at 37 $^{\circ}$C for 5, 15, 30, 60 and 120 min. After the specified time of incubating micelles with BT549-Luc and T47D cells, the medium containing micelles was removed, and the cells were rinsed three times with cold PBS, and completely dissolved in DMSO. The fluorescent intensity of doxorubicin at excitation 485 nm and emmission 590 nm wavelength indicating DOX encapsulated micelles bound to the cells was measured by using a fluorescence microplate reader (Spectramax M3e).

Statistical analysis

Statistical evaluation of data was performed using an analysis of variance (one-way ANOVA). Newman–Keuls was used as a post-hoc test to assess the significance of differences. To compare the significance of the difference between the means of two groups, a *t*-test was performed; in all cases, a value of $p < 0.05$ was accepted as significant.

5. Results and discussion

Computational peptide-protein binding

To target cancer cells, we need a peptide that can interact strongly with human MUC1 protein. James et al have identified several peptides that can bind respectively to two fragments cut out from MUC1[25]. However, binding to the fragments of MUC1 does not necessarily indicate binding to MUC1 protein as a whole because the fragments may adopt different conformations when they are in the protein and cut out. Moreover, to deliver drugs, the candidate peptides need to be ligated with a short linker peptide GGGSK or GGGSC. With these extra amino acids, the extended candidate peptide may not be able to bind even the cut-out fragments. Therefore, an in-house computational pipeline is used to select the extended peptides that can still bind MUC1 protein tightly. To this end, both MUC1 structure and the peptide structures are required. However as a membrane protein, MUC1 structure is difficult to be solved, and thus has no crystal structures available for our purpose. To overcome this, I-TASSER as the most accurate predictor is used to predict the structures of MUC1 and the extended peptides. Subsequently, Hex is used to measure the binding affinities between the MUC1 structure and the candidate peptides, respectively. Structures are measured by Hex. As a result, the candidate peptides are ranked decreasing in binding affinities to MUC1: QNDRHPRGGGSK-FITC, HSQLPQVGGGSK-FITC, PHETPHQGGGSK-FITC, DPQVNPAGGGSK-FITC, HATRHTTGGGSK-FITC, PGSEHKHGGGSK-FITC and TNTLSNNGGGSK-FITC. The peptide with highest affinity (QNDRHPR-GGGSKFITC) is predicted to interact with residues 94W, 95G, 96Q and 97D in MUC1. These residues are in one of the MUC1 fragments used in the binding experiments by James et al. This consistency suggests that QNDRHPRGGGSK-FITC is a promising lead peptide. Similar consistency is also observed in the peptide ranked the second highest (HSQLPQVGGGSK-FITC), whereas the lowly ranked peptides are not predicted as strong binder to MUC1. Nevertheless, we picked the two strongest binders and the weakest binder for the following experimental validations.

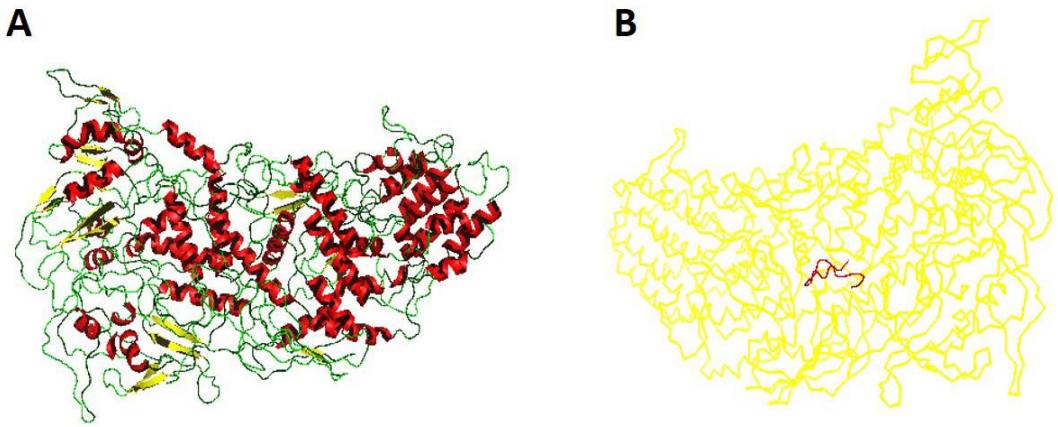

Fig.1 (A) Predicted structure of MUC1 (B) Predicted structure of MUC1 binding peptide

Preparation of micelle copolymer

Lithocholic acid has good biocompatibility and high structural rigidity base on its steroid skeleton[26]. Meanwhile, octadecyl amine provide extended hydrophobic block for increased drug loading. In addition, PEG segment will provide hydrophilic sheath surrounding the core, once micelle formed, that was expected to improved circulation time. Pegylated octadecyl lithocholate was synthesized using multiple reactions. Octadecyl lithocholate was synthesized with moderate yield (62.3 ± 20.1%). Succinyl octadecyl lithocholate and pegylated octadecyl lithocholate were synthesized with relatively high yield (91.9 ± 13.9 and 88.3 ± 7.1%). FTIR spectra were recorded to monitor changes in chemical structure of polymer conjugates. The conversion of hydroxyl group of octadecyl lithocholate to carboxyl group on succinyl octadecyl lithocholate was confirmed by the disappearance of vibration of hydroxyl group (O-H) ~3320 cm^{-1}. The product also had a new peak at 1729 cm^{-1} suggesting the formation of ester carbonyl group. Octadecyl lithocholate: C=O (1655 cm^{-1}), C-H (2849, 2920 cm^{-1}), O-H (3322, 3431 cm^{-1}). Succinyl octadecyl lithocholate: C=O (1648, 1729 cm^{-1}), C-O (2360 cm^{-1}), C-H (2850, 2917 cm^{-1})

MUC1 expression on BT549-Luc and T47D breast carcinoma cells

MUC1 expression on BT549-Luc and T47D carcinoma cells was assessed by standard Western blot analysis. Both of BT549 and T47D cells express the MUC-1 protein. When compare between both cell types, the expression level of MUC-1 in T47D cells was 4 times higher than that in BT549 cells (Fig. 2).

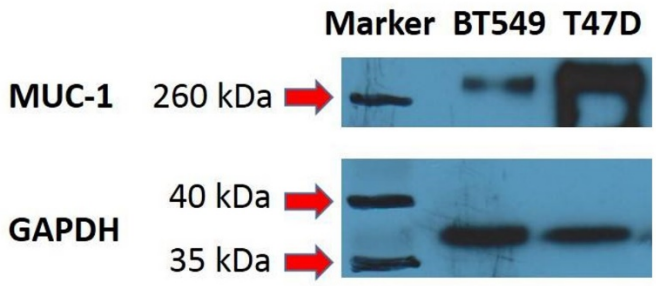

Fig.2 MUC1 expression in breast cancer cell lines, BT549-Luc and T47D

Preparation of fluorescence labeled MUC1 targeting peptides

From computational protein-peptide binding experiment, top two binders (QND and HSQ) and the worst binder (TNT) were chosen to be synthesized. The peptides were synthesized manually using standard Fmoc solid phase peptide synthesis, and purified using semi-preparative HPLC. Retention time on analytical HPLC of QND-FITC, HSQ-FITC, and TNT-FITC peptides were 13.9, 16.2 and 18.3 min, respectively (Fig. 3). Purity of QND-FITC, HSQ-FITC, and TNT-FITC peptides were 84.7, 89.5, and 75.3%, respectively, on analytical HPLC. The exact molecular mass of QND-FITC, HSQ-FITC, and TNT-FITC peptides using MS were 1696.8, 1582.7, and 1537.6 g/mol, respectively.

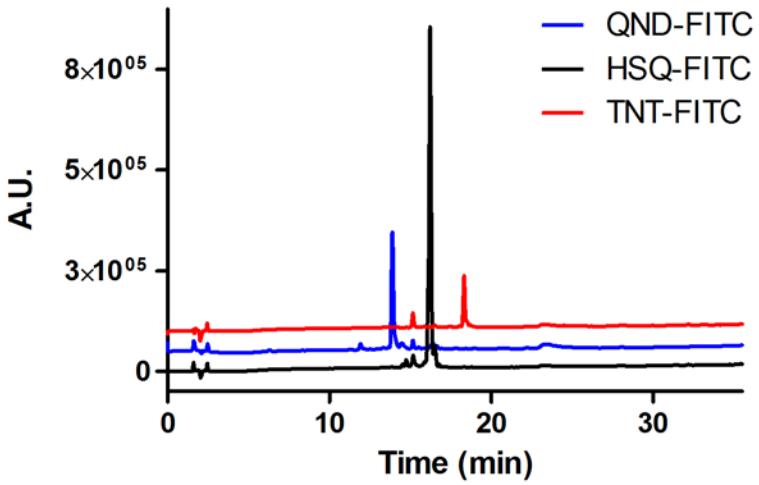

Fig. 3 Purity of fluorescent peptides, QND-FITC, HSQ-FITC, and TNT-FITC, using analytical HPLC

Binding of QND, HSQ, and TNT peptides to BT549-Luc and T47D cells

Cellular binding of FITC conjugated QND, HSQ, and TNT peptides were compared by analyzing fluorescent intensity of micrographs acquired by fluorescence microscopy. Figure 4A showed that the fluorescent intensity of cells after incubation with FITC conjugated QND and HSQ peptides with BT-549 cells was significantly higher than that of TNT peptide. The result suggested that QND and HSQ peptides bound BT549-Luc cells more rapidly and with a greater extent than TNT peptide (Figure 4). As shown in Figure 4B, Image analysis of mean fluorescent intensity shows that FITC conjugated QND and HSQ peptides exhibited a significant higher degree of binding after incubation with BT549-Luc cells at 37^{O}C for 60 min as compared to TNT peptide.

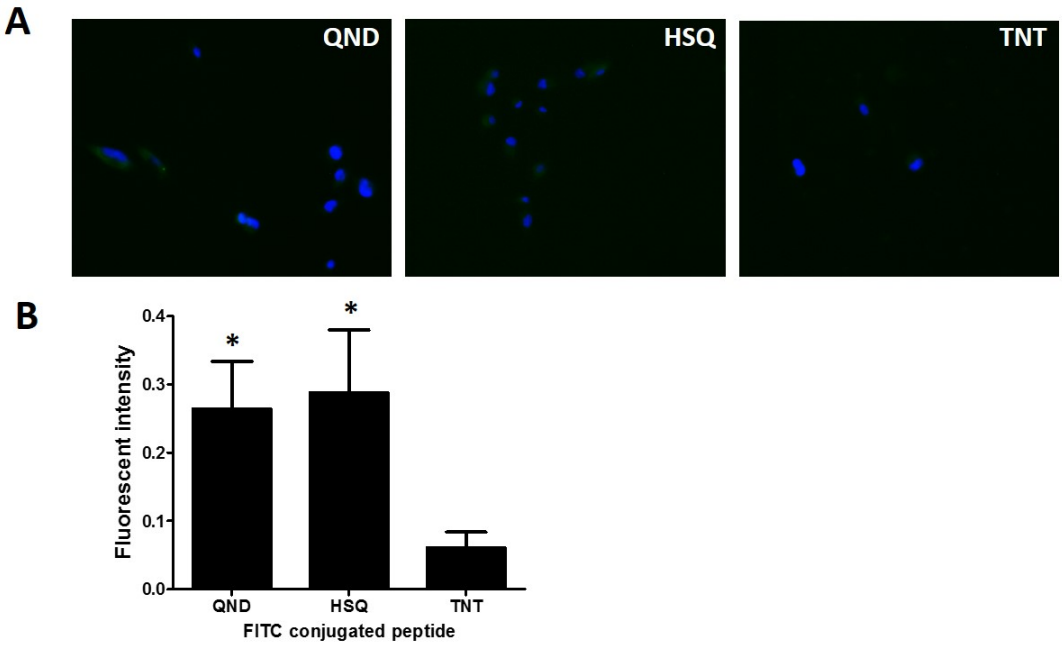

Fig. 4 (A) Representative fluorescence images of specific peptide binding on BT549-Luc cells for QND, HSQ and TNT after 60 min of incubation at 37°C (B) Image analysis of mean fluorescent intensity of specific peptide binding on BT-549 cells shows differences in fluorescence staining intensity (* = p <0.05).

Preparation of DOX loaded micelles

The copolymer pegylated octadecyl lithocholate spontaneously self-assembled into core-shell-structural micelle. We observed a critical micelle concentration of 110.5, 55.1, and 98.9 μM for untargeted, QHD, and HSQ micelles, respectively, on fluorescence probe study using pyrene (Fig. 5A). Dynamic light scattering showed that the size of DOX micelles was approximately 300-320 nm in diameter with a moderate polydispersity (Table 1). The particle size distribution was bimodal where the smaller size was 60-70 nm and the bigger size was 400-500 nm, suggesting aggregation of the micelle. The size of the micelles measured on DLS was consistent with that seen on TEM (Fig. 6). TEM images showed spherical particles of the micelles. The zeta potential value of DOX micelles was about -3 to 4.5 mV (Table 1). An increase in surface charge after conjugation with QND and HSQ

peptides was observed, which was expected due to the *pI* value of QND and HSQ peptides (8.58 and 7.67, respectively).

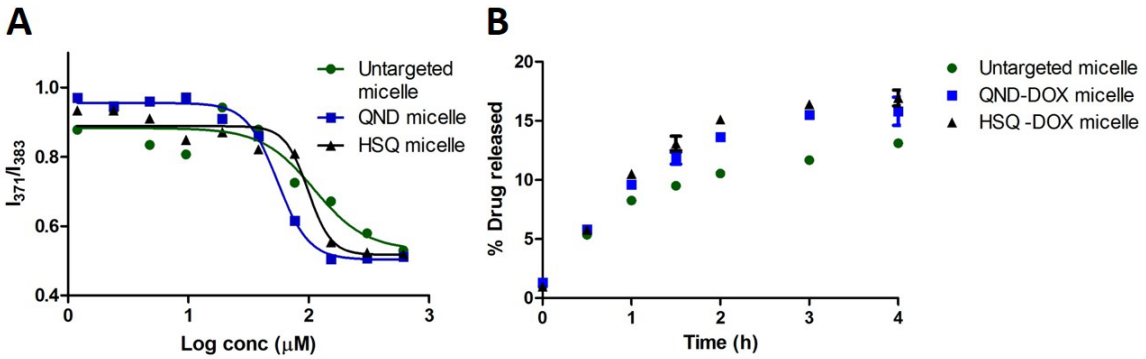

Fig. 5 (A) Critical micelle concentration (CMC) of non-targeted, QND, and HSQ micelles (B) Release profile of DOX from untargeted DOX, QND-DOX, and HSQ-DOX micelles at pH 7

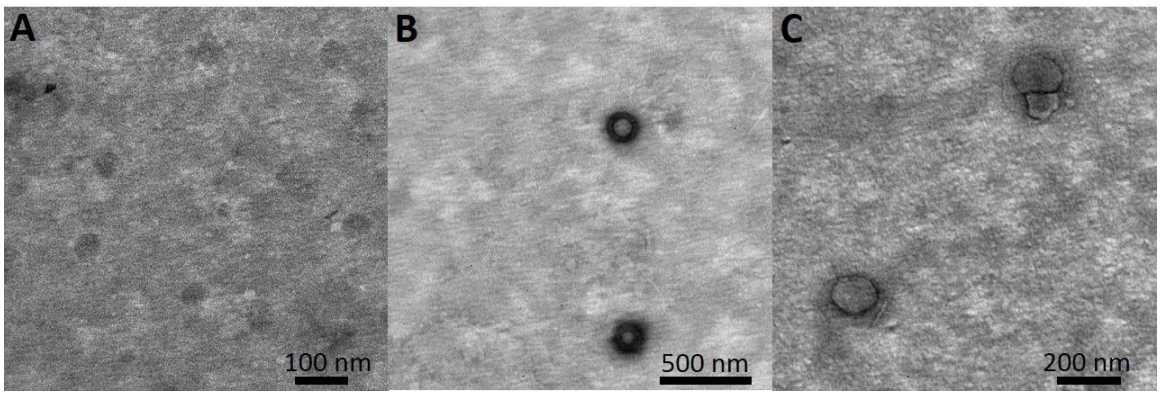

Fig. 6 Transmission electron micrograph (TEM) of DOX (A), QND-DOX (B), and HSQ-DOX (C) micelles showing spherical morphology

Table 1 Micelle characterization including diameter on dynamic light scattering (DLS), polydispersity index (PDI), zeta potential (surface charge), and DOX entrapment efficiency (%EE)

Sample	Diameter (nm)	Zeta potential (mV)	PDI	%EE
DOX micelle	319.7 ± 34.9	-3.0 ± 2.9	0.523 ± 0.086	71.0 ± 8.7
QND-DOX micelle	300.6 ± 36.5	4.5 ± 0.4	0.423 ± 0.031	86.0 ± 3.6
HSQ-DOX micelle	319.3 ± 12.2	1.6 ± 0.6	0.412 ± 0.061	92.7 ± 5.2

The entrapment efficiency of micelles was measured by fluorescence spectroscopy using a microplate reader. The entrapment efficiencies of DOX in untargeted DOX, QND-DOX, and HSQ-DOX micelle were relatively high, 71.0±8.7, 86.0±3.6, and 92.7±5.2 %, respectively. Entrapment efficiency of DOX in nanoparticles can range from low to high. For example, DOX was loaded ranging from 1.3 to 4.4% using poly(Ɛ-caprolactone)-PEG micelle that has hydrophobic block length 2.5-24.7 kDa[27]. In another study, DOX entrapment efficiency was 55.6-64.3% using DOX-PEG-alendronate micelles[28]. Generally, drug hydrophobicity plays a critical role in drug-loading process. However, other parameters affecting drug loading are polymer crystallinity and hydrogen bonding interaction between drug and polymer[27]. DOX is intrinsically less hydrophobic owing to its polar hydroxyl and amino groups. Therefore, DOX loading could vary.

The release profile of DOX from DOX loaded micelles in phosphate buffer pH 7 was shown in Fig. 5B. DOX was released from DOX micelles in similar amount with no initial burst release and showing prolonged release profile. In 4 h, DOX was released from untargeted, QND-DOX, and HSQ-DOX micelles 13.1, 15.8, and 16.9%, respectively. The majority of loaded DOX was still immobilized in micelle core after 4 h.

Cytotoxicity assay

The cytotoxicity of free DOX, DOX, QND-DOX, and HSQ-DOX micelles to BT549-Luc and T47D was evaluated by using MTT assay. The IC_{50} value of free DOX, DOX released from untargeted, QND, and HSQ micelle was 4.3, 4.4, 1.75, and 3.75 μM, respectively, in BT549-Luc cells (Fig. 7A-D). The IC_{50} value of free DOX, DOX released from untargeted, QND, and HSQ micelle was 5.2, 4.2, 4.6, and 4 μM, respectively, in T47D cells (Fig. 7E-H). The cytotoxicity of DOX released from micelles was comparable to that of free DOX, P=0.39 by Kruskal-Wallis test, on both cells. The relative IC_{50} value of DOX from each micelle formulation suggested that the activity of drug encapsulated in micelle was not affected by encapsulation.

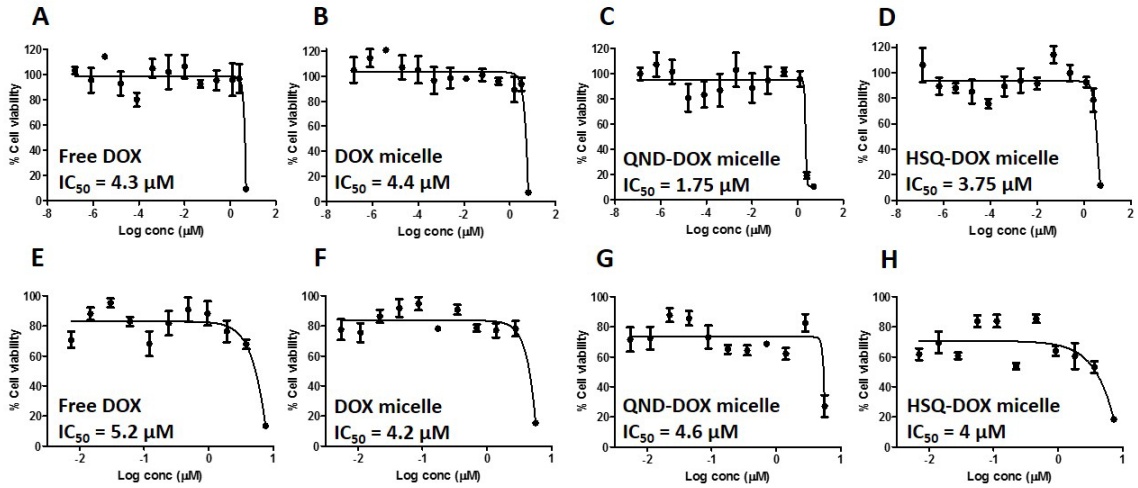

Fig. 7 Cytotoxicity of free DOX, DOX, QND-DOX, and HSQ-DOX micelles on BT549-Luc (A-D) and T47D (E-H) cells

Quantification of binding and uptake of QND-DOX-micelles and HSQ-DOX-micelles to BT549-Luc and T47D cells

Since QND and HSQ have been shown to bind BT549-Luc cells, these two peptides were used to further determine the targeting efficiency of micelles encapsulating DOX. Within the first hour, the binding extent of QND-DOX-micelles and HSQ-DOX-micelles to BT-549 cells was found to be

significantly higher than untargeted DOX-micelles (Figure 8A). The fluorescent intensity was increased concomitantly with incubation time, suggesting an increasing amount of QND-DOX-micelles and HSQ-DOX-micelles bound or were taken up by cells along with the incubation time. HSQ-DOX-micelles bound BT549-Luc cells greater than QND-DOX-micelles in 60 and 120 min. At 120 min, the binding of HSQ-DOX-micelles was increased up to 3.2 fold compared to untargeted micelles.

T47D cells were incubated with QND-DOX-micelles, HSQ-DOX-micelles, and untargeted DOX-micelles to further assess the specificity of binding mediated by QND or HSQ. QND and HSQ resulted in 1.2 – 1.9 times enhancement of binding and uptake of DOX in T47D cells (Figure 8B). This

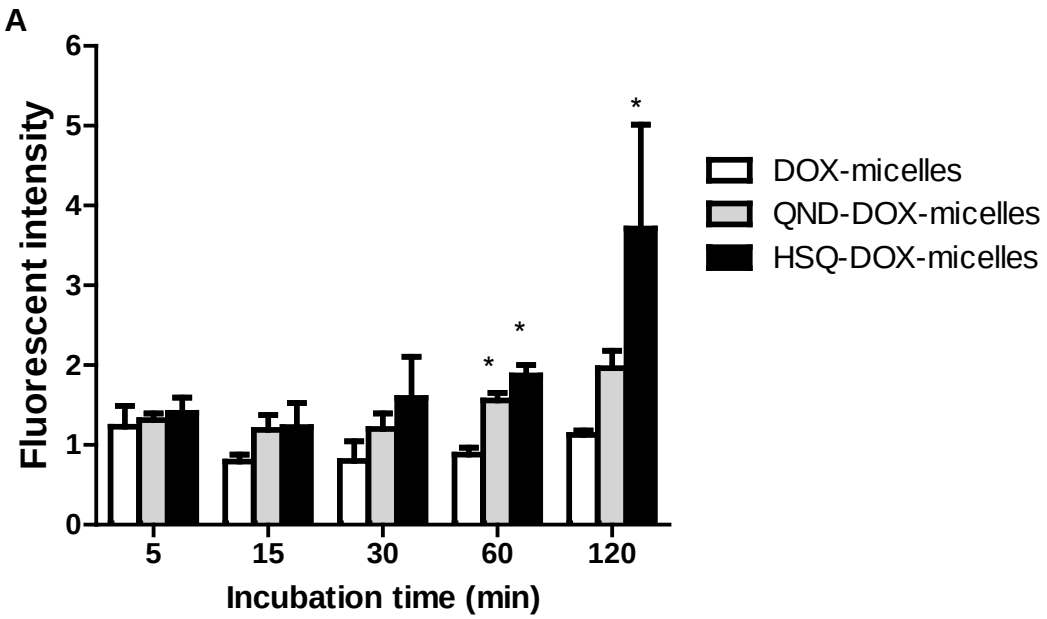

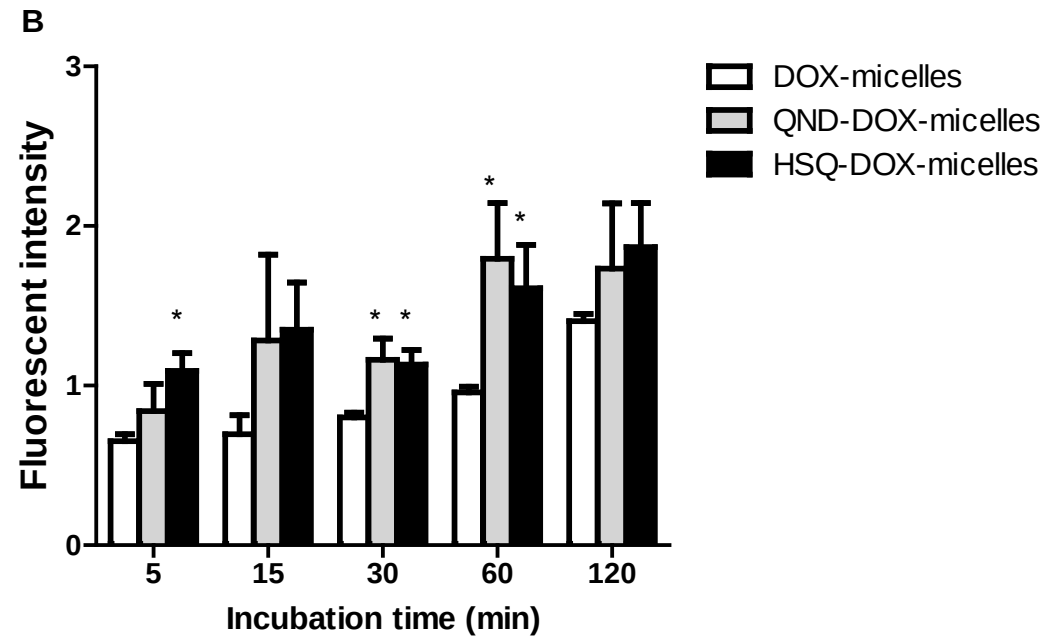

observation was consistent with the results observed in BT549-Luc cells. Increasing the incubation

Fig. 8 (A) Binding and uptake of untargeted, QND and HSQ conjugated DOX-micelles to BT549-Luc cells. (B) Binding and uptake of untargeted, QND and HSQ conjugated DOX-micelles to T47D cells * indicated $p<0.05$ compared to DOX-micelles.

time increased the binding and uptake of the micelles up to 60 min. At 120 min of incubation, the fluorescent intensity of cells was not significantly different from untargeted micelles suggesting ligand binding saturation.

6. Conclusion

QND and HSQ peptides have been shown to bind MUC1 protein using computational docking. These two peptide were subsequently tested and showing superior binding on MUC1 expressing breast cancer cell, BT549-Luc. Hence, they were chosen to be grafted onto pegylated octadecyl lithocholate copolymer acting as targeting moieties. Targeted pegylated octadecyl lithocholate DOX micelles were then successfully formulated having mean hydrodynamic diameter around 300-320 nm. These micelles have octadecyl lithocholate core capable of encapsulating DOX with relatively high drug entrapment efficiency. The in vitro release data indicated prolonged release profile at pH 7. Compared to free DOX, the targeted micelles showed comparable cytotoxicity in BT549-Luc and T47D cells. Binding and uptake study showed that QND-DOX and HSQ-DOX micelles bound BT549-Luc and T47D cells greater than untargeted DOX micelle. Taken together, QND-DOX and HSQ-DOX micelles had potential in treating triple negative breast cancer.

7. Output (Acknowledge the Thailand Research Fund)

7.1 International Journal Publication

Under submission to Molecular Pharmaceutics journal.

Title: Specific targeting of MUC1 overexpressing breast carcinoma cells with doxorubicin-loaded micelles

Authors: Supang Khondee[1], Chuda Chittasupho[2], Singkome Tima[3], and Songyot Anuchapreeda[3,*]

Affiliations:

[1]School of Pharmaceutical Sciences, University of Phayao, Phayao, Thailand

[2]Faculty of Pharmacy, Srinakharinwirot University, Rangsit-Nakhonnayok Rd., Ongkarak, Nakhonnayok, Thailand

[3]Division of Clinical Microscopy, Department of Medical Technology, Faculty of Associated Medical Sciences, Chiang Mai University, Chiang Mai, Thailand

***Correspondence:**

Songyot Anuchapreeda

Associate Professor

Division of Clinical Microscopy,

Department of Medical Technology,

Faculty of Associated Medical Sciences,

Chiang Mai University, Chiang Mai, 50200, THAILAND

Office: 66-53-949237

Fax: 66-53-945066

Email: sanuchapreeda@gmail.com, songyot.anuch@cmu.ac.th

Abstract

Breast cancer is the leading cause of cancer death among women. The human mucin1 protein (MUC1) is overexpressed in approximately 90% of human breast cancers. In order to increase therapeutic effect of a model drug, doxorubicin (DOX), on breast cancer, DOX loaded micelles that target MUC1 was developed. The micelle was self-assembled using copolymer pegylated octadecyl lithocholate as an amphiphilic platform. MUC1 targeting peptides, QND and HSQ, were identified and conjugated on micelles. The size and drug entrapment efficiency of untargeted, QND-DOX and HSQ-DOX micelles were 320, 300 and 319 nm and 71, 86 and 93%, respectively. Critical micelle concentration (CMC) of untargeted, QND, and HSQ micelle were 110.5, 55.1, and 98.9 μM, respectively. In 4 h, DOX was released 13.1, 15.8 and 16.9 %, respectively, from untargeted, QND-DOX and HSQ-DOX micelles in pH 7 buffer. The IC_{50} of untargeted DOX, QND-DOX and HSQ-DOX micelles on BT549-Luc and T47D cells were comparable to that of free DOX. Additionally, we observed significantly greater binding and uptake of QND-DOX and HSQ-DOX micelles on BT549-Luc and T47D cells compared to untargeted DOX micelle. These results suggested that QND-DOX and HSQ-DOX micelles had potential application in triple negative breast cancer treatment.

Keywords: human mucin1 protein (MUC1); targeted therapy; breast cancer; doxorubicin; micelles

Introduction

Breast cancer is the most frequent diagnosed cancer and the leading cause of cancer death among females worldwide[1]. It is a heterogeneous disease encompassing multiple subgroups with differing molecular signatures, prognoses, and responses to therapies.[2] From the clinical view point, breast cancer can be subdivided into three major subtypes: tumors expressing estrogen receptors (ERs) and/or progesterone receptors (PRs) (commonly referred to as hormone receptor-positive [HR-positive] tumors), ERBB2-amplified (also known as human epidermal receptor 2-amplified [HER2-amplified] breast cancer, and the remaining group commonly referred to as triple-negative breast cancer (TNBC) due to lack of expression of the ERs and PRs and normal or negative HER2 expression.[3] There has been growing interest in targeting therapy to improve the effectiveness of breast cancer treatment. Since 2005, HER2 has been used as an effective target for trastuzumab much as steroid hormone receptors are targets for endocrine therapies, while other targets are under exploration. However, chemotherapy is the mainstay of adjuvant treatment of patients with TNBC, which is an aggressive disease lacking a historical therapeutic target. Chemotherapeutic agents including doxorubicin, paclitaxel, cyclophosphamide, methotrexate, and fluorouracil are also frequently used in preoperative treatment.[4] Despite the success of these anti-cancer drugs against cancers, their use can be severely limited by their life-threatening toxicities including cardiac toxicity, neuropathy, neutropenia, myelosuppression, and acute renal failure.[5-8]

Doxorubicin (DOX) is one of the most potent and widely used in cancer treatment. It works by inhibiting nucleic acid synthesis within cancer cells. Doxorubicin has a number of undesirable side effects such as cardiac toxicity and myelosuppression that leads to a very narrow therapeutic index. Doxil®, PEGylated liposomal doxorubicin, is “passively targeted” to tumor via enhanced permeability and retention (EPR) effect. Its doxorubicin is released and become available to tumor cells by as yet unknown means.[9] Even though, Doxil® has lower dose-limiting toxicity than doxorubicin[10], two side effects which are not typically observed for free drug doxorubicin treatment have been reported. The first one is grade 2 or 3 desquamating dermatitis and is referred to as Palmer Plantar Erythrodysthesia (PPE) or “foot and hand syndrome”. The second effect is an infusion-related reaction that shows up as flushing and shortness of breath.[11] Other technologies for doxorubicin delivery such as synthetic polymeric conjugates[12] and antibody targeted carriers[13] have demonstrated reduced or altered toxicity in Phase 1 trials, yet the therapeutic efficacy of these formulations has yet to be demonstrated. In the absence of safer and efficacious systemic formulations, targeted doxorubicin micelle is an alternative therapeutic and may offer improve tolerability and improve efficacy.

The human mucin1 protein (MUC1), a membrane-bound glycoprotein, belongs to a class of high molecular weight (>400 kDa) O-linked glycoprotein.[14] A major function of the ectodomains of these membrane-tethered mucins is to hydrate and lubricate cell surfaces. MUC1 is expressed at the luminal membrane of most glandular and ductal epithelial cells. MUC1 has a large, highly glycosylated extracellular domain that consists mainly of numerous peptide repeats and a short cytoplasmic tail. MUC1 is overexpressed in approximately 90% of human breast cancers. It is also overexpressed in many other

human tumors such as colorectal, pancreatic and ovarian cancers. High-level mucin expression causes loss of cellular polarity, interferes with cell adhesion, protects tumor from being killed by the host immune system, as well as by chemotherapeutic agents, thus favoring metastases.[14] Tumor-associated MUC1 has short carbohydrate side chains and exposes epitopes on its peptide core. Given its abundance and overexpression in many adenocarcinomas, and the post-translational alteration in glycosylation pattern, therefore, MUC1 has been investigated as a potential target for cancer therapies. To date, there are currently no MUC1-targeted therapies in clinical use, while several MUC1 therapies are in clinical trials. Thus, MUC1 targeted doxorubicin micelle formulation is worth exploring and could potentially improve the efficacy of MUC1-expressing cancer treatments.

Different targeting ligands have been explored to target chemotherapeutic agents to breast cancer cells. For example, engineered antibodies[15-17], tumor-homing peptides[18], and aptamer[19]. Among these approaches, antibodies have received a lot of attention for a number of years. However, the level of success in cancer targeting has been limited because of their large size, possible immunogenicity, production cost, low physicochemical stability, and short *in vivo* half-life.[20] Peptides are smaller, have excellent tissue penetration properties, and can easily be chemically conjugated with drugs and oligonucleotide. Therefore, the use of peptide as targeting ligands has attracted considerable attention. In this study, the specific binding of several MUC1 targeting peptides on MUC1 expressing breast cancer cell lines was examined. The top two targeting peptides were then conjugated to micelle platform. DOX loaded targeting micelles were formulated followed by drug entrapment efficiency, release, and cytotoxicity assessments. The binding and uptake of DOX loaded targeting micelles were then evaluated on BT549-Luc and T47D breast cancer cells.

Experimental section

Materials

Human breast carcinoma cells (BT549-Luc and T47D) were obtained from the ATCC (Manassas, VA). Dulbecco's modified Eagle's medium (DMEM) was obtained from GIBCO. Phosphate-buffered saline (PBS) was obtained from Amresco, and penicillin-streptomycin was obtained from Capricorn scientific. Fetal bovine serum (FBS) was obtained from PAA laboratories. BT549-Luc and T47D were grown in DMEM. Cells were maintained according to ATCC guidelines.

Lithocholic acid, N,N'-diisopropylcarbodiimde (DIC), N-hydroxysuccinimide (NHS), and pyrene were obtained from Sigma. Succinic anhydride, 4-(dimethylamino) pyridine (DMAP), N,N-diisopropylethylamine (DIEA) were obtained from Merck. Octadecyl amine and fluorescein isothiocyanate (FITC) were obtained from Acros. N-(3-dimethylaminopropyl)-N'-ethylcarbodiimide HCl (EDC) was obtained from Fluka. Tris (2-carboxyethyl) phosphine HCl (TCEP) was obtained from Thermo Scientific and 3-[4,5-dimethylthiazol-2-yl]-2,5 diphenyl tetrazolium bromide (MTT) was obtained from AppliChem. Doxorubicin was purchased from LC Laboratories. Methoxy PEG_{3K} amine and maleiimide $PEG_{3.5K}$ amine were obtained from JenKem Technology. Fmoc-amino acids, Boc amino acids, o-benzotriazole-N,N,N′,N′-

tetramethyluronium hexafluorophosphate (HBTU) and 1-Hydroxybenzotriazole (HOBt) and rink amide MBHA resin were obtained from Aapptec. Dialysis membranes with molecular weight cut off (MWCO) of 12-14 kDa were obtained from Spectrum Laboratories, Inc. All reagents were used as received.

Identification of peptides bound by MUC1 protein using computational methods

A computational pipeline to predict peptides that efficiently bind MUC1 protein was set up. In the pipeline, I-TASSER with default parameters was used to predict the structure of MUC1 protein. As a result, the software provided five MUC1 model structures, and the first model is usually the most accurate one. Thus, the first model was used as the structure of MUC1 protein in our study. In the same way, the structures of the candidate peptides was determined. Hex was used to infer the binding affinity between MUC1 protein and the candidate peptides, respectively. For each peptide, Hex docked it into the MUC1 structure based on Fast Fourier Transform (FFT), and calculated the *p*-value of the docking result. The *p*-value indicates how well the peptide and the protein fit each other. Thus, the p-value was used as a proxy of binding affinity between the peptide and the MUC1 structure.

Determination of MUC1 expression using western blot analysis

The expression level of MUC-1 protein (CD227) in various cell types was evaluated using Western blot analysis. The whole protein extracts from BT549-Luc and T47D cells were prepared using RIPA buffer (50 mM Tris-HCl, 150 mM NaCl, 1% Triton X-100, 0.5 mM ethylenediaminetetraacetic acid (EDTA), and 0.1% sodium dodecyl sulfate (SDS)) containing protease inhibitors. The protein concentration was measured by the Folin-Lowry method. Then, the proteins at 50 μg were separated by 7.5% SDS-PAGE. The analysis for MUC-1 protein was performed using primary mouse anti-human MUC-1 (BioLegend Inc., San Diego, CA, USA) in the ratio 1:1000, followed by a treatment with HRP-conjugated anti-mouse IgG (Promaga, WI, USA) in the ratio 1:15000 dilution. The GAPDH protein was probed with primary rabbit polyclonal anti-GAPDH (Santa Cruz Biotechnology, CA, USA) in the ratio 1:1000, followed by treatment with HRP-conjugated goat anti-rabbit IgG in a 1:20000 dilution (Promega, WI, USA). The protein bands were visualized using the Luminata Forte Western HRP substrate (Merck Millipore Corporation, MA, USA) and quantified by ChemiDoc XRS (Bio-Rad, CA, USA)

Synthesis and purification of fluorescence labeled MUC1 targeting peptides for in vitro peptide selection

The panel of candidate peptides (QNDRHPR-GGGSK, HSQLPQV-GGGSK and TNTLSNN-GGGSK) were synthesized manually using solid phase peptide synthesis with standard Fmoc chemistry. Fluorescein isothiocyanate (FITC) was conjugated at the C-terminus on the side chain of a lysine residue via the GGGSK linker. Resins (~0.03 mmol) were swelled in DMF (1 mL). In a separate tube, FITC (0.045 mmol) was dissolved in DMF (0.6 mL). ~23 μL of DIEA (46 μL, 0.26 mmol) was added to both tubes. FITC solution was added to the resins. The reaction was allowed to stir 2-3 days at room temperature. The resins were washed and cleaved. The resulting peptides were precipitated in cold diethyl ether. The

peptides were then purified using a semi-preparative HPLC (Shimadzu) with water-acetonitrile gradient mobile phase containing 0.1% trifluoroacetic acid (TFA). The resulting peptides were lyophilized and characterized with an ESI mass spectrometer (MicrOTOF mass spectrometer, Bruker Daltonics). Peptides purity was determined on analytical HPLC.

Peptide synthesis for micelle conjugation

The QNDRHPR-GGGSC and HSQLPQV-GGGSC peptides were selected for micelle labeling, and synthesized as described above. At C terminal, cysteine (C) was introduced to make free thiol group after cleavation. This thiol group is for conjugation to maleiimide PEG octadecyl lithocholate to form peptide-copolymer conjugate. Resins were washed, cleaved, and the resulting peptide was precipitated in cold diethyl ether. The resulting peptides were lyophilized. The peptide was then purified using a semi-preparative HPLC and characterized with an ESI mass spectrometer.

Fluorescence microscopy study of binding and uptake of QND, HSQ and TNT peptides

BT549-Luc cells were seeded in cell culture chamber slide and incubated overnight to allow cell attachment. The culture medium was removed and washed one time with PBS. The cells were incubated with 0.5% BSA in PBS for 30 min at 4°C to block non-specific binding. The cells were then incubated with FITC conjugated QND, HSQ and TNT peptides dissolved in serum-free DMEM for 60 min at 37 °C, 5% CO_2 and were washed three times with PBS to remove unbound peptides. The cells were fixed in 4% paraformaldehyde. To visualize nuclei, cells were incubated with 2 μg/ml Hoechst33342 for 15 min at room temperature, washed three times with PBS, and examined under fluorescence microscope. Fluorescence micrographs were acquired using Nikon Eclipse TS100-F and NIS-Elements, version 4.0 software.

Synthesis of micelles

Octadecyl lithocholate

Lithocholic acid (1.5 g, 4 mmol) and HOBt (1.5 g, 10 mmol) were dissolved in N,N-dimethylformamide (DMF) (12 mL). DIC (1.5 mL, 10 mmol) was added. After 10 min for activation, octadecyl amine (0.9 g, 3.3 mmol) was added along with dichloromethane (DCM) 4 mL, and the reaction was allowed to stir overnight at room temperature (RT). The resulting product was filtered and vacuum dried.

Succinyl octadecyl lithocholate

Octadecyl lithocholate (573 mg, 0.91 mmol) was dissolved in anhydrous DCM (15 mL). Catalytic amount of DMAP was added. Succinic anhydride (90.9 mg, 0.91 mmol) and DIEA (950 μL, 5.45 mmol) were then added and the reaction was allowed to run overnight at RT. The solvent was evaporated under N_2 and the resulting product was vacuum dried.

Pegylated octadecyl lithocholate

Succinyl octadecyl lithocholate (128 mg, 0.18 mmol) was dissolved in DCM 2.5 ml and DMF 1 mL. HOBt (78 mg, 0.54 mmol) was added, following by adding DIC (84 µL, 0.54 mmol). Methoxy PEG amine (300 mg, 0.1 mmol) was added after 10 min for activation. The reaction was allowed to stir overnight at 40^{o}C. The solvent was partially removed under N_2 and the resulting product was precipitated in cold diethyl ether, centrifuged, and vacuum dried. Succinyl octadecyl lithocholate was conjugated with maleimide PEG amine in the same manner.

Thiol peptide and maleimide pegylated octadecyl lithocholate conjugation

Maleimide pegylated octadecyl lithocholate (335 mg, 0.08 mmol) and TCEP (19 mg, 0.07 mmol) were dissolved in phosphate buffer pH 8.0 (15 mL). Thiol peptide (0.07 mmol) was added and the reaction was allowed to run overnight at RT. The resulting product was dialyzed against three changes of water and lyophilized.

Fourier Transform Infrared (FTIR) spectrometry

FTIR spectra were recorded on a FT-IR spectrometer (Nicolet iS5, Thermo Scientific) to monitor changes in chemical structure of polymer conjugates. Samples were prepared in potassium bromide (KBr) discs and spectra were recorded in the range of 4000-400 cm^{-1}.

Micelle preparation

The micelles were prepared by dissolving pegylated octadecyl lithocholate and/or QND pegylated octadecyl lithocholate or HSQ pegylated octadecyl lithocholate in PBS. For targeted micelle, optimal peptide density (50%) was selected to present on micelle surface based on previous studies[21, 22]. Polymers were sonicated ~30 min or until fully dispersed. Doxorubicin (10 mg/mL) basic stock solution was added to the polymer solution. DOX feeding amount was 1.5% w/w of polymer used. The solution was sonicated for 5 min. Then micelle solution was centrifuged at 8000 rpm for 10 min to remove insoluble material. Doxorubicin micelles in supernatant were separated. For all experiments, 1.6 mM of polymer was used.

Dynamic Light Scattering (DLS)

Hydrodynamic diameters and surface charges of micelles were determined on a Mavern nanosizer (Nano-ZS90) with a 4 mW linear polarized laser (633 nm He-Ne). Samples were studied at 25^{o}C and in 10 mm diameter polystyrene cells. The hydrodynamic diameters were calculated from the Stoked-Einstein equation. Measurements were made in triplicate with independently prepared samples, and variability was reported as ±standard deviation.

Transmission Electron Microscopy (TEM)

TEM images were obtained on a transmission electron microscope (JEOL JEM-2010). Samples were prepared onto copper grids with 1% uranyl acetate (negative staining).

Critical micelle concentration (CMC)

Micelles form spontaneously at the critical micelle concentration (CMC). Pyrene was dissolved in

acetone (24 mM) and aliquots of stock solution were added to 1.5 mL eppendorf tubes to provide a final pyrene concentration of 6 μM. Acetone was evaporated and replaced with untargeted, QND, and HSQ micelles prepared with serial dilution (01.2-2450 μM). Solutions were incubated at 55^{o}C overnight and left at RT for 3 hours prior to the experiment. We measured the fluorescence intensity of pyrene at I_1 = 371 nm and I_3 = 383 nm over a range of concentrations of untargeted, QND, and HSQ micelles on a microplate reader.[23] The intensity ratios of I_1 to I_3 were plotted as a function of logarithm of micelle concentration (log μM). The CMC value was taken from the intersection of the tangent to the curve at the inflection with the horizontal tangent through the points at concentrations.[24]

Entrapment efficiency (EE)

The amount of doxorubicin was determined by a microplate reader (Synergy H1, BioTek). Two hundred microliters of micelle solution was transferred to a black 96-well plate prior to reading. The entrapment efficiency (%EE) was calculated according to the following equation:

Entrapment efficiency (%EE) = $\frac{amount\ of\ encapsulated\ doxorubicin\ (\mu g)\ in\ micelles}{amount\ of\ added\ doxorubicin\ (\mu g)\ during\ formulation}$ x 100.

Release study

The release of DOX from DOX loaded micelles was investigated by using dialysis method. Briefly, micelle solutions were prepared at concentration 1.6 mM. Doxorubicin was encapsulated ~1.5% (w/w) in micelles, and 3 mL of each formulation was transferred into 12,000 Da MWCO dialysis bag (Spectrum laboratories Inc.) (*n*=3). Dialysis bags were immerged in 100 mL of phosphate buffer at pH 7, and the release medium was stirred to facilitate drug release. The experiment was run at room temperature. At fixed time points, aliquots were taken, and drug concentrations were measured by a microplate reader. Release medium was added after each sampling.

Cytotoxicity

Cytotoxicity was determined by measuring growth inhibition for a panel of cells (BT549-Luc and T47D) on an MTT assay. Cell viability was calculated based on a comparison of untreated cells and those treated with free DOX and with DOX, QND-DOX, and HSQ-DOX micelles under the same conditions. The panel of cells were harvested and seeded at a density of 2.5x10^4 cells/well in 96-well plates. Cells were cultured for 24 hours prior to adding doxorubicin micelles in serial dilution. Free doxorubicin at equivalent doses was incubated with cells in the same manner. After 1 day of incubation, the medium was removed, cells were washed twice with PBS, and MTT solution (10 μL, 5 mg/mL) was added to each well. After an additional 4 hours of incubation, MTT solution was removed. Formazan crystals produced by live cells were solubilized in DMSO and the absorbance was measured at 570 nm (test) and 630 nm (reference) using a microplate reader. Cytotoxicity of tested substance was presented as the half maximal inhibitory concentration (IC_{50}). At the concentration, the test substance inhibits cell viability by 50%.

Quantification of binding specificity and uptake of QND-DOX-micelles and HSQ-DOX-micelles

BT549-Luc and T47D cells were seeded in 96-well plate at a cell concentration of 80,000 cells/ml. QND-DOX-micelles and HSQ-DOX-micelles containing 16 μg/mL of DOX were suspended in serum free DMEM (2.5 mg/ml, 100 μl) and incubated with the cells at 37 °C for 5, 15, 30, 60 and 120 min. After the specified time of incubating micelles with BT549-Luc and T47D cells, the medium containing micelles was removed, and the cells were rinsed three times with cold PBS, and completely dissolved in DMSO. The fluorescent intensity of doxorubicin at excitation 485 nm and emmission 590 nm wavelength indicating DOX encapsulated micelles bound to the cells was measured by using a fluorescence microplate reader (Spectramax M3e).

Statistical analysis

Statistical evaluation of data was performed using an analysis of variance (one-way ANOVA). Newman–Keuls was used as a post-hoc test to assess the significance of differences. To compare the significance of the difference between the means of two groups, a *t*-test was performed; in all cases, a value of $p < 0.05$ was accepted as significant.

Results and discussion

Computational peptide-protein binding

To target cancer cells, we need a peptide that can interact strongly with human MUC1 protein. James et al have identified several peptides that can bind respectively to two fragments cut out from MUC1[25]. However, binding to the fragments of MUC1 does not necessarily indicate binding to MUC1 protein as a whole because the fragments may adopt different conformations when they are in the protein and cut out. Moreover, to deliver drugs, the candidate peptides need to be ligated with a short linker peptide GGGSK or GGGSC. With these extra amino acids, the extended candidate peptide may not be able to bind even the cut-out fragments. Therefore, an in-house computational pipeline is used to select the extended peptides that can still bind MUC1 protein tightly. To this end, both MUC1 structure and the peptide structures are required. However as a membrane protein, MUC1 structure is difficult to be solved, and thus has no crystal structures available for our purpose. To overcome this, I-TASSER as the most accurate predictor is used to predict the structures of MUC1 and the extended peptides. Subsequently, Hex is used to measure the binding affinities between the MUC1 structure and the candidate peptides, respectively. Structures are measured by Hex. As a result, the candidate peptides are ranked decreasing in binding affinities to MUC1: QNDRHPRGGGSK-FITC, HSQLPQVGGGSK-FITC, PHETPHQGGGSK-FITC, DPQVNPAGGGSK-FITC, HATRHTTGGGSK-FITC, PGSEHKHGGGSK-FITC and TNTLSNNGGGSK-FITC. The peptide with highest affinity (QNDRHPR-GGGSKFITC) is predicted to interact with residues 94W, 95G, 96Q and 97D in MUC1. These residues are in one of the MUC1 fragments used in the binding experiments by James et al. This consistency suggests that QNDRHPRGGGSK-FITC is a promising lead peptide. Similar consistency is also observed in the peptide ranked the second highest (HSQLPQVGGGSK-FITC), whereas the lowly ranked peptides are not predicted as strong binder to

MUC1. Nevertheless, we picked the two strongest binders and the weakest binder for the following experimental validations.

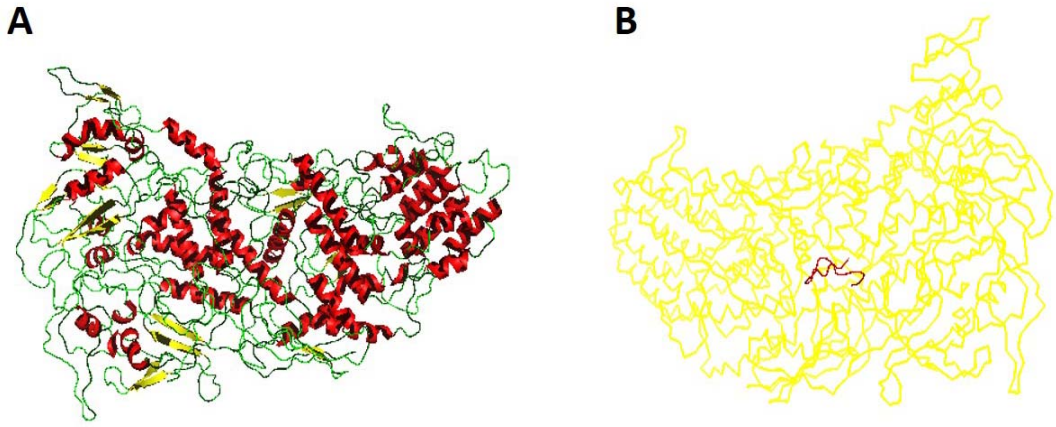

Fig.1 (A) Predicted structure of MUC1 (B) Predicted structure of MUC1 binding peptide

Preparation of micelle copolymer

Lithocholic acid has good biocompatibility and high structural rigidity base on its steroid skeleton[26]. Meanwhile, octadecyl amine provide extended hydrophobic block for increased drug loading. In addition, PEG segment will provide hydrophilic sheath surrounding the core, once micelle formed, that was expected to improved circulation time. Pegylated octadecyl lithocholate was synthesized using multiple reactions. Octadecyl lithocholate was synthesized with moderate yield (62.3 ± 20.1%). Succinyl octadecyl lithocholate and pegylated octadecyl lithocholate were synthesized with relatively high yield (91.9 ± 13.9 and 88.3 ± 7.1%). FTIR spectra were recorded to monitor changes in chemical structure of polymer conjugates. The conversion of hydroxyl group of octadecyl lithocholate to carboxyl group on succinyl octadecyl lithocholate was confirmed by the disappearance of vibration of hydroxyl group (O-H) ~3320 cm^{-1}. The product also had a new peak at 1729 cm^{-1} suggesting the formation of ester carbonyl group. Octadecyl lithocholate: C=O (1655 cm^{-1}), C-H (2849, 2920 cm^{-1}), O-H (3322, 3431 cm^{-1}). Succinyl octadecyl lithocholate: C=O (1648, 1729 cm^{-1}), C-O (2360 cm^{-1}), C-H (2850, 2917 cm^{-1})

MUC1 expression on BT549-Luc and T47D breast carcinoma cells

MUC1 expression on BT549-Luc and T47D carcinoma cells was assessed by standard Western blot analysis. Both of BT549 and T47D cells express the MUC-1 protein. When compare between both cell types, the expression level of MUC-1 in T47D cells was 4 times higher than that in BT549 cells (Fig. 2).

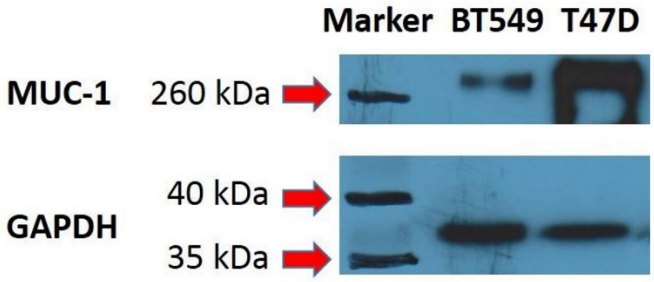

Fig.2 MUC1 expression in breast cancer cell lines, BT549-Luc and T47D

Preparation of fluorescence labeled MUC1 targeting peptides

From computational protein-peptide binding experiment, top two binders (QND and HSQ) and the worst binder (TNT) were chosen to be synthesized. The peptides were synthesized manually using standard Fmoc solid phase peptide synthesis, and purified using semi-preparative HPLC. Retention time on analytical HPLC of QND-FITC, HSQ-FITC, and TNT-FITC peptides were 13.9, 16.2 and 18.3 min, respectively (Fig. 3). Purity of QND-FITC, HSQ-FITC, and TNT-FITC peptides were 84.7, 89.5, and 75.3%, respectively, on analytical HPLC. The exact molecular mass of QND-FITC, HSQ-FITC, and TNT-FITC peptides using MS were 1696.8, 1582.7, and 1537.6 g/mol, respectively.

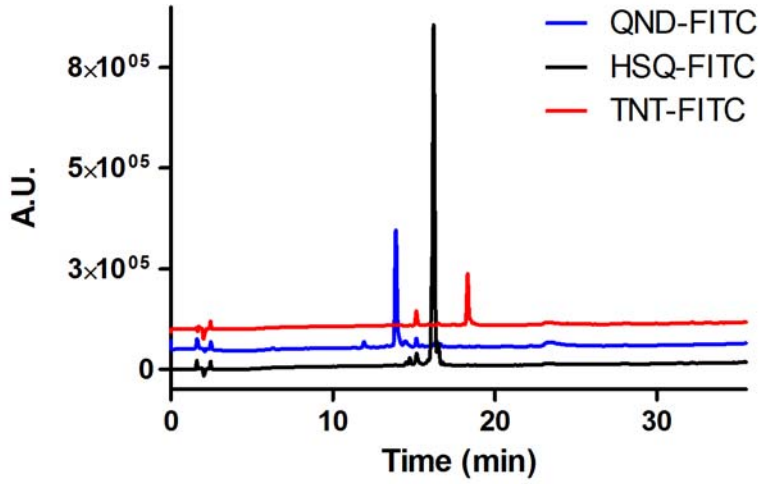

Fig. 3 Purity of fluorescent peptides, QND-FITC, HSQ-FITC, and TNT-FITC, using analytical HPLC

Binding of QND, HSQ, and TNT peptides to BT549-Luc and T47D cells

Cellular binding of FITC conjugated QND, HSQ, and TNT peptides were compared by analyzing fluorescent intensity of micrographs acquired by fluorescence microscopy. Figure 4A showed that the fluorescent intensity of cells after incubation with FITC conjugated QND and HSQ peptides with BT-549 cells was significantly higher than that of TNT peptide. The result suggested that QND and HSQ peptides

bound BT549-Luc cells more rapidly and with a greater extent than TNT peptide (Figure 4). As shown in Figure 4B, Image analysis of mean fluorescent intensity shows that FITC conjugated QND and HSQ peptides exhibited a significant higher degree of binding after incubation with BT549-Luc cells at 37°C for 60 min as compared to TNT peptide.

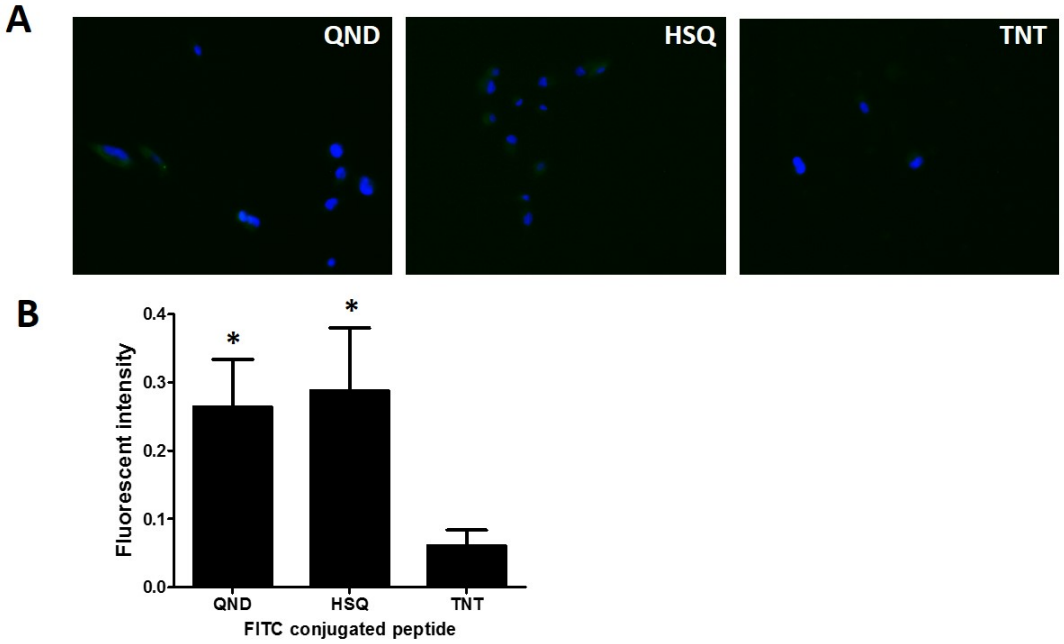

Fig. 4 (A) Representative fluorescence images of specific peptide binding on BT549-Luc cells for QND, HSQ and TNT after 60 min of incubation at 37°C (B) Image analysis of mean fluorescent intensity of specific peptide binding on BT-549 cells shows differences in fluorescence staining intensity (* = p <0.05).

Preparation of DOX loaded micelles

The copolymer pegylated octadecyl lithocholate spontaneously self-assembled into core-shell-structural micelle. We observed a critical micelle concentration of 110.5, 55.1, and 98.9 μM for untargeted, QHD, and HSQ micelles, respectively, on fluorescence probe study using pyrene (Fig. 5A). Dynamic light scattering showed that the size of DOX micelles was approximately 300-320 nm in diameter with a moderate polydispersity (Table 1). The particle size distribution was bimodal where the smaller size was 60-70 nm and the bigger size was 400-500 nm, suggesting aggregation of the micelle. The size of the micelles measured on DLS was consistent with that seen on TEM (Fig. 6). TEM images showed spherical particles of the micelles. The zeta potential value of DOX micelles was about -3 to 4.5 mV (Table 1). An increase in surface charge after conjugation with QND and HSQ peptides was observed, which was expected due to the *pI* value of QND and HSQ peptides (8.58 and 7.67, respectively).

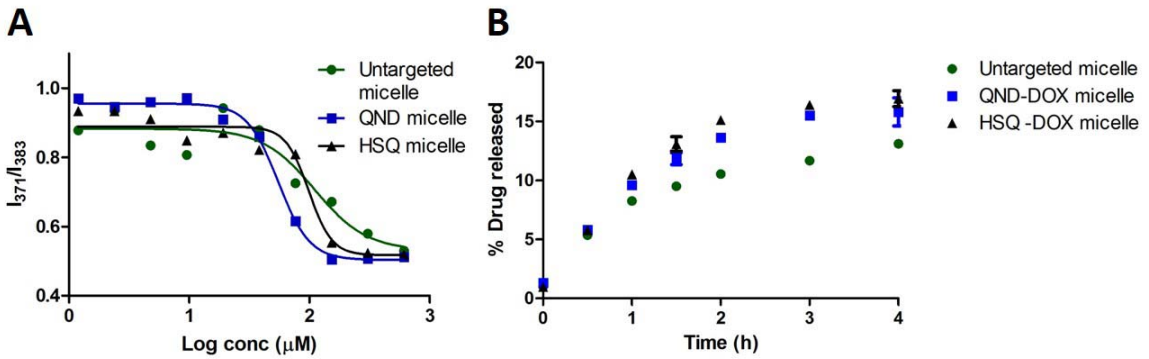

Fig. 5 (A) Critical micelle concentration (CMC) of non-targeted, QND, and HSQ micelles (B) Release profile of DOX from untargeted DOX, QND-DOX, and HSQ-DOX micelles at pH 7

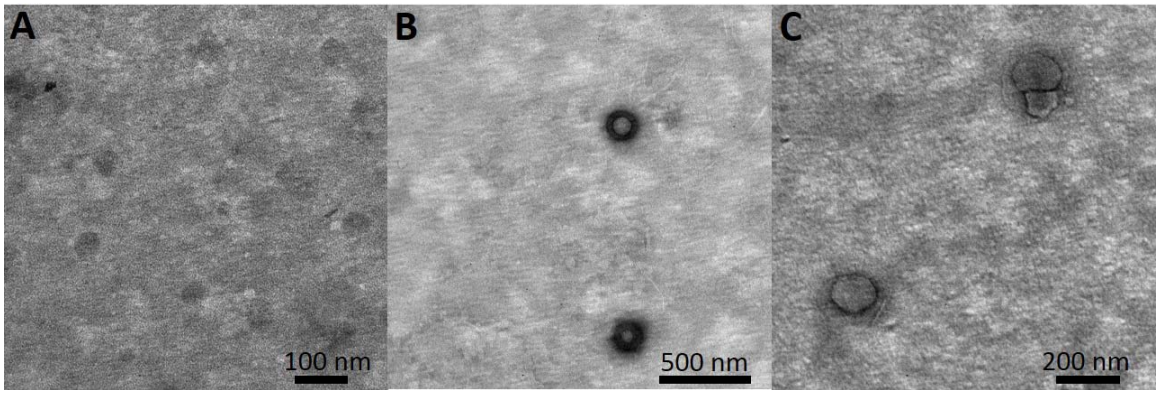

Fig. 6 Transmission electron micrograph (TEM) of DOX (A), QND-DOX (B), and HSQ-DOX (C) micelles showing spherical morphology

Table 1 Micelle characterization including diameter on dynamic light scattering (DLS), polydispersity index (PDI), zeta potential (surface charge), and DOX entrapment efficiency (%EE)

Sample	Diameter (nm)	Zeta potential (mV)	PDI	%EE
DOX micelle	319.7 ± 34.9	-3.0 ± 2.9	0.523 ± 0.086	71.0 ± 8.7
QND-DOX micelle	300.6 ± 36.5	4.5 ± 0.4	0.423 ± 0.031	86.0 ± 3.6
HSQ-DOX micelle	319.3 ± 12.2	1.6 ± 0.6	0.412 ± 0.061	92.7 ± 5.2

The entrapment efficiency of micelles was measured by fluorescence spectroscopy using a microplate reader. The entrapment efficiencies of DOX in untargeted DOX, QND-DOX, and HSQ-DOX micelle were relatively high, 71.0±8.7, 86.0±3.6, and 92.7±5.2 %, respectively. Entrapment efficiency of DOX in nanoparticles can range from low to high. For example, DOX was loaded ranging from 1.3 to 4.4% using poly(ε-caprolactone)-PEG micelle that has hydrophobic block length 2.5-24.7 kDa[27]. In another study, DOX entrapment efficiency was 55.6-64.3% using DOX-PEG-alendronate micelles[28]. Generally, drug hydrophobicity plays a critical role in drug-loading process. However, other parameters affecting drug loading are polymer crystallinity and hydrogen bonding interaction between drug and polymer[27]. DOX is

intrinsically less hydrophobic owing to its polar hydroxyl and amino groups. Therefore, DOX loading could vary.

The release profile of DOX from DOX loaded micelles in phosphate buffer pH 7 was shown in Fig. 5B. DOX was released from DOX micelles in similar amount with no initial burst release and showing prolonged release profile. In 4 h, DOX was released from untargeted, QND-DOX, and HSQ-DOX micelles 13.1, 15.8, and 16.9%, respectively. The majority of loaded DOX was still immobilized in micelle core after 4 h.

Cytotoxicity assay

The cytotoxicity of free DOX, DOX, QND-DOX, and HSQ-DOX micelles to BT549-Luc and T47D was evaluated by using MTT assay. The IC_{50} value of free DOX, DOX released from untargeted, QND, and HSQ micelle was 4.3, 4.4, 1.75, and 3.75 μM, respectively, in BT549-Luc cells (Fig. 7A-D). The IC_{50} value of free DOX, DOX released from untargeted, QND, and HSQ micelle was 5.2, 4.2, 4.6, and 4 μM, respectively, in T47D cells (Fig. 7E-H). The cytotoxicity of DOX released from micelles was comparable to that of free DOX, P=0.39 by Kruskal-Wallis test, on both cells. The relative IC_{50} value of DOX from each micelle formulation suggested that the activity of drug encapsulated in micelle was not affected by encapsulation.

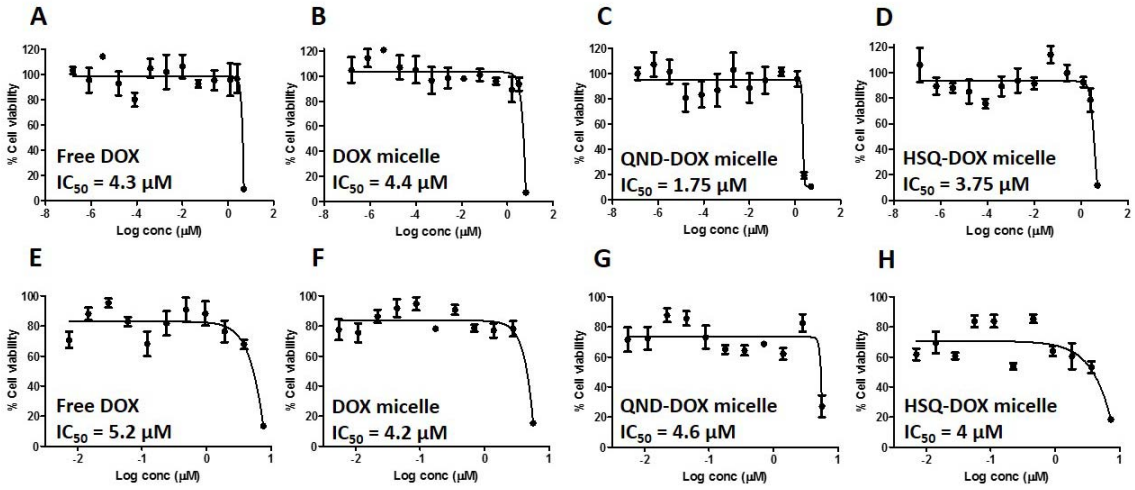

Fig. 7 Cytotoxicity of free DOX, DOX, QND-DOX, and HSQ-DOX micelles on BT549-Luc (A-D) and T47D (E-H) cells

Quantification of binding and uptake of QND-DOX-micelles and HSQ-DOX-micelles to BT549-Luc and T47D cells

Since QND and HSQ have been shown to bind BT549-Luc cells, these two peptides were used to further determine the targeting efficiency of micelles encapsulating DOX. Within the first hour, the binding extent of QND-DOX-micelles and HSQ-DOX-micelles to BT-549 cells was found to be significantly higher than untargeted DOX-micelles (Figure 8A). The fluorescent intensity was increased concomitantly

with incubation time, suggesting an increasing amount of QND-DOX-micelles and HSQ-DOX-micelles bound or were taken up by cells along with the incubation time. HSQ-DOX-micelles bound BT549-Luc cells greater than QND-DOX-micelles in 60 and 120 min. At 120 min, the binding of HSQ-DOX-micelles was increased up to 3.2 fold compared to untargeted micelles.

T47D cells were incubated with QND-DOX-micelles, HSQ-DOX-micelles, and untargeted DOX-micelles to further assess the specificity of binding mediated by QND or HSQ. QND and HSQ resulted in 1.2 – 1.9 times enhancement of binding and uptake of DOX in T47D cells (Figure 8B). This observation was consistent with the results observed in BT549-Luc cells. Increasing the incubation time increased the binding and uptake of the micelles up to 60 min. At 120 min of incubation, the fluorescent intensity of cells was not significantly different from untargeted micelles suggesting ligand binding saturation.

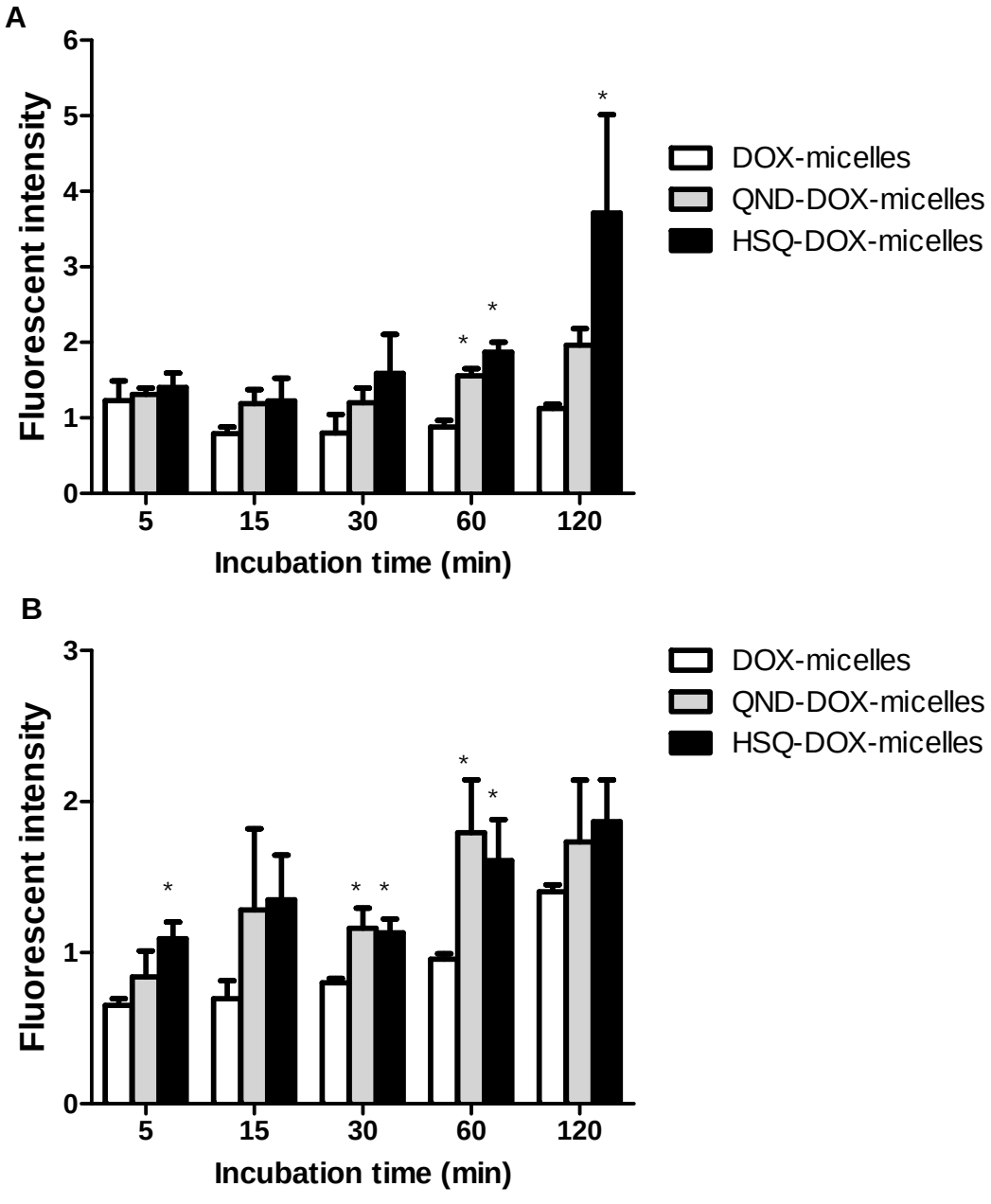

Fig. 8 (A) Binding and uptake of untargeted, QND and HSQ conjugated DOX-micelles to BT549-Luc cells. (B) Binding and uptake of untargeted, QND and HSQ conjugated DOX-micelles to T47D cells * indicated $p<0.05$ compared to DOX-micelles.

Conclusions

QND and HSQ peptides have been shown to bind MUC1 protein using computational docking. These two peptide were subsequently tested and showing superior binding on MUC1 expressing breast cancer cell, BT549-Luc. Hence, they were chosen to be grafted onto pegylated octadecyl lithocholate copolymer acting as targeting moieties. Targeted pegylated octadecyl lithocholate DOX micelles were then successfully formulated having mean hydrodynamic diameter around 300-320 nm. These micelles have octadecyl lithocholate core capable of encapsulating DOX with relatively high drug entrapment efficiency. The in vitro release data indicated prolonged release profile at pH 7. Compared to free DOX, the targeted micelles showed comparable cytotoxicity in BT549-Luc and T47D cells. Binding and uptake study showed that QND-DOX and HSQ-DOX micelles bound BT549-Luc and T47D cells greater than untargeted DOX micelle. Taken together, QND-DOX and HSQ-DOX micelles had potential in treating triple negative breast cancer.

Acknowledgments

This research was supported by the Thailand Research Fund (TRF) and University of Phayao TRG5780051 to SK.

References

1. Jemal, A.; Bray, F.; Center, M. M.; Ferlay, J.; Ward, E.; Forman, D. Global cancer statistics. *CA: a cancer journal for clinicians* 2011, *61*, (2), 69-90.
2. Sorlie, T.; Perou, C. M.; Tibshirani, R.; Aas, T.; Geisler, S.; Johnsen, H.; Hastie, T.; Eisen, M. B.; van de Rijn, M.; Jeffrey, S. S. Gene expression patterns of breast carcinomas distinguish tumor subclasses with clinical implications. *Proceedings of the National Academy of Sciences* 2001, *98*, (19), 10869-10874.
3. Higgins, M. J.; Baselga, J. Targeted therapies for breast cancer. *The Journal of clinical investigation* 2011, *121*, (10), 3797.
4. Gianni, L.; Eiermann, W.; Semiglazov, V.; Manikhas, A.; Lluch, A.; Tjulandin, S.; Zambetti, M.; Vazquez, F.; Byakhow, M.; Lichinitser, M. Neoadjuvant chemotherapy with trastuzumab followed by adjuvant trastuzumab versus neoadjuvant chemotherapy alone, in patients with HER2-positive locally advanced breast cancer (the NOAH trial): a randomised controlled superiority trial with a parallel HER2-negative cohort. *The Lancet* 2010, *375*, (9712), 377-384.
5. Ayhanci, A.; Yaman, S.; Appak, S.; Gunes, S. Hematoprotective effect of seleno-L-methionine on cyclophosphamide toxicity in rats. *Drug and Chemical Toxicology* 2009, *32*, (4), 424-428.
6. Bergmann, T. K.; Gr√©en, H.; Brasch-Andersen, C.; Mirza, M. R.; Herrstedt, J. r.; H√∏lund, B.; du Bois, A.; Damkier, P.; Vach, W.; Brosen, K. Retrospective study of the impact of pharmacogenetic variants on paclitaxel toxicity and survival in patients with ovarian cancer. *European journal of clinical pharmacology* 2011, *67*, (7), 693-700.
7. Cai, S.; Thati, S.; Bagby, T. R.; Diab, H.-M.; Davies, N. M.; Cohen, M. S.; Forrest, M. L. Localized doxorubicin chemotherapy with a biopolymeric nanocarrier improves survival and reduces toxicity in xenografts of human breast cancer. *Journal of Controlled Release* 2010, *146*, (2), 212-218.
8. Schmiegelow, K. Advances in individual prediction of methotrexate toxicity: a review. *British journal of haematology* 2009, *146*, (5), 489-503.

9. Barenholz, Y. C. Doxil, The first FDA-approved nano-drug: Lessons learned. *Journal of controlled release* 2012, *160*, (2), 117-134.
10. Wang, A. Z.; Langer, R.; Farokhzad, O. C. Nanoparticle delivery of cancer drugs. *Annual review of medicine* 2012, *63*, 185-198.
11. Barenholz, Y. C. Doxil¬Æ‚ÄîThe first fda-approved nano-drug: Lessons learned. *Journal of controlled release* 2012, *160*, (2), 117-134.
12. B. Rihova, J. S., J. Prausova, K. Kubackova, M. Jelinkova, L. Rozprimova, M. Sirova, D. Plocova, T. Etrych, V. Subr, T. Mrkvan, M. Kovar, K. Ulbrich,. Cytostatic and immunomobilizing activities of polymer-bound drugs: experimental and first clinical data. *Journal of controlled release* 2003, *91*, (1), 1-16.
13. Tolcher, A. W.; Sugarman, S.; Gelmon, K. A.; Cohen, R.; Saleh, M.; Isaacs, C.; Young, L.; Healey, D.; Onetto, N.; Slichenmyer, W. Randomized phase II study of BR96-doxorubicin conjugate in patients with metastatic breast cancer. *Journal of clinical oncology* 1999, *17*, (2), 478-478.
14. von Mensdorff-Pouilly, S.; Snijdewint, F.; Verstraeten, A.; Verheijen, R.; Kenemans, P. Human MUC1 mucin: a multifaceted glycoprotein. *The International journal of biological markers* 2000, *15*, (4), 343.
15. Kirpotin, D. B.; Drummond, D. C.; Shao, Y.; Shalaby, M. R.; Hong, K.; Nielsen, U. B.; Marks, J. D.; Benz, C. C.; Park, J. W. Antibody targeting of long-circulating lipidic nanoparticles does not increase tumor localization but does increase internalization in animal models. *Cancer research* 2006, *66*, (13), 6732-6740.
16. Nielsen, U. B.; Kirpotin, D. B.; Pickering, E. M.; Hong, K.; Park, J. W.; Refaat Shalaby, M.; Shao, Y.; Benz, C. C.; Marks, J. D. Therapeutic efficacy of anti-ErbB2 immunoliposomes targeted by a phage antibody selected for cellular endocytosis. *Biochimica et Biophysica Acta (BBA)-Molecular Cell Research* 2002, *1591*, (1), 109-118.
17. Park, J. W.; Hong, K.; Kirpotin, D. B.; Colbern, G.; Shalaby, R.; Baselga, J.; Shao, Y.; Nielsen, U. B.; Marks, J. D.; Moore, D. Anti-HER2 immunoliposomes enhanced efficacy attributable to targeted delivery. *Clinical Cancer Research* 2002, *8*, (4), 1172-1181.
18. Mathews, A. S.; Ahmed, S.; Shahin, M.; Lavasanifar, A.; Kaur, K. Peptide Modified Polymeric Micelles Specific for Breast Cancer Cells. *Bioconjugate chemistry* 2013, *24*, (4), 560-570.
19. Savla, R.; Taratula, O.; Garbuzenko, O.; Minko, T. Tumor targeted quantum dot-mucin 1 aptamer-doxorubicin conjugate for imaging and treatment of cancer. *Journal of Controlled Release* 2011, *153*, (1), 16-22.
20. Aina, O. H.; Liu, R.; Sutcliffe, J. L.; Marik, J.; Pan, C.-X.; Lam, K. S. From combinatorial chemistry to cancer-targeting peptides. *Molecular pharmaceutics* 2007, *4*, (5), 631-651.
21. Fakhari, A.; Baoum, A.; Siahaan, T. J.; Le, K. B.; Berkland, C. Controlling ligand surface density optimizes nanoparticle binding to ICAM‚Äê1. *Journal of pharmaceutical sciences* 2011, *100*, (3), 1045-1056.
22. Khondee, S.; Rabinsky, E. F.; Owens, S. R.; Joshi, B. P.; Qiu, Z.; Duan, X.; Zhao, L.; Wang, T. D. Targeted therapy of colorectal neoplasia with rapamycin in peptide-labeled pegylated octadecyl lithocholate micelles. *Journal of Controlled Release* 2015, *199*, 114-121.
23. Goddard, E.; Turro, N.; Kuo, P.; Ananthapadmanabhan, K. Fluorescence probes for critical micelle concentration determination. *Langmuir* 1985, *1*, (3), 352-355.
24. Cavalieri, F.; Chiessi, E.; Paradossi, G. Chaperone-like activity of nanoparticles of hydrophobized poly (vinyl alcohol). *Soft Matter* 2007, *3*, (6), 718-724.
25. James, T. C.; Bond, U. Molecular Mimics of the Tumour Antigen MUC1. *PloS one* 2012, *7*, (11), e49728.
26. Matsusaki, M.; Thi, T. H.; Kaneko, T.; Akashi, M. Enhanced effects of lithocholic acid incorporation into liquid-crystalline biopolymer poly (coumaric acid) on structural ordering and cell adhesion. *Biomaterials* 2005, *26*, (32), 6263-6270.
27. Shuai, X.; Ai, H.; Nasongkla, N.; Kim, S.; Gao, J. Micellar carriers based on block copolymers of poly (Œµ-caprolactone) and poly (ethylene glycol) for doxorubicin delivery. *Journal of Controlled Release* 2004, *98*, (3), 415-426.
28. Ye, W.-l.; Zhao, Y.-p.; Li, H.-q.; Na, R.; Li, F.; Mei, Q.-b.; Zhao, M.-g.; Zhou, S.-y. Doxorubicin-poly (ethylene glycol)-alendronate self-assembled micelles for targeted therapy of bone metastatic cancer. *Scientific reports* 2015, *5*.